# Heat transfer characteristics of near-pseudocritical nitrogen in vertical small tubes—a new empirical correlation

Wang, Yi; Lu, Tiejun; Yang, Ren; Sciacovelli, Adriano; Ding, Yulong; Li, Yongliang

*DOI:*
10.1016/j.ijthermalsci.2022.108001



*Document Version*
Publisher's PDF, also known as Version of record

*Citation for published version (Harvard):*
Wang, Y, Lu, T, Yang, R, Sciacovelli, A, Ding, Y & Li, Y 2023, 'Heat transfer characteristics of near-pseudocritical nitrogen in vertical small tubes—a new empirical correlation', *International Journal of Thermal Sciences*, vol. 184, 108001. https://doi.org/10.1016/j.ijthermalsci.2022.108001

International Journal of Thermal Sciences 184 (2023) 108001

Contents lists available at ScienceDirect

International Journal of Thermal Sciences

journal homepage: www.elsevier.com/locate/ijts

# Heat transfer characteristics of near-pseudocritical nitrogen in vertical small tubes—a new empirical correlation

Yi Wang, Tiejun Lu, Ren Yang, Adriano Sciacovelli, Yulong Ding, Yongliang Li *

*School of Chemical Engineering, University of Birmingham, Birmingham, B15 2TT, UK*

ARTICLE INFO

*Keywords:*
Cryogenic fluid
Supercritical nitrogen
Vertical circular tube
Pseudo-critical point
Internal flow convection
Heat transfer coefficient correlation

ABSTRACT

This experimental study aims to investigate the characteristics of supercritical nitrogen ($N_2$) internal flow convective heat transfer. A series of heat transfer experiments were conducted with $N_2$ flowing upwardly in a uniformly heated vertical circular bare stainless steel tube (4.57 mm ID) under pressures of 3.5 and 4 MPa that beyond its critical pressure (3.4 MPa), mass fluxes of 27.9, 38.1, 50.8 kg/m$^2$-s, and heat fluxes of 8.1, 9.3, 11.2 kW/m$^2$, respectively. Experimental results demonstrate that supercritical $N_2$ behaves similarly as other supercritical fluids such as water and $CO_2$, both thermally and hydrodynamically, when transforming from subcritical to supercritical conditions in a heated vertical tube. In the vicinity of pseudo-critical point, the local convective heat transfer coefficient of $N_2$ first elevated to a maximum peak value and then deteriorated as the fluid temperature becomes higher than pseudo-critical temperature. In general, the convective heat transfer coefficient increases with mass flux due to enhanced turbulence but decreased with pressure and heat flux, which can be attributed to the unique thermo-physical property variations of $N_2$ near its pseudo-critical point. Furthermore, a new heat transfer correlation has been developed in this study exclusively for internal flow convective heat transfer of supercritical $N_2$ flowing upwardly in a small circular bare tube based on the experimental results. It has been shown that the newly proposed heat transfer correlation can well predict, within ±15%, the corresponding heat transfer data of supercritical $N_2$ while the heat transfer correlations in the literature constructed for other supercritical fluids (e.g. water and $CO_2$) fail to do so. The new correlation inherits the basic form of Dittus-Boelter correlation, but takes extra considerations of fluid thermo-physical property differences between the heated tube wall and bulk fluid core and uses Eckert number to divide the whole heat transfer process into three regions around the pseudo-critical point. The results of this study also suggest that the research on internal flow convective heat transfer of supercritical $N_2$ (e.g. continue to perfect the heat transfer correlation) should not stop and a more complete database covering a wider range of experimental conditions is needed to prepare the future blossom of supercritical $N_2$ as one of the primary cryogenic heat transfer fluids.

## 1. Introduction

A supercritical fluid is a fluid whose temperature and pressure are beyond the critical values, and as a result, distinct vapor and liquid phases will no longer exist in the fluid. Thermo-physical properties of supercritical fluids, such as specific heat, thermal conductivity, density and viscosity significantly change as the fluids transform from subcritical to supercritical. Consequently, supercritical fluids can effuse through porous solids like a gas, breaking the mass transfer limitations for liquid transporting pass such materials. In addition, when close to the pseudo-critical point, small adjustments in pressure or temperature may lead to dramatic variations in fluid's thermo-physical properties, allowing the properties of the supercritical fluid to be fine-tuned according to desired applications. Hence, the relevance of supercritical fluid has been rising in many important fields due to their unique thermodynamic and rheological properties. For example, supercritical fluids have been employed as the energy carriers in advanced power cycles [1–3]; supercritical fluids have been applied to facilitate material processing for fuel cells [4–6]; supercritical fluids such as supercritical helium and nitrogen have had huge impacts on the development of cryogenic technology [7,8,13]. Accordingly, the internal flow convective heat transfer of supercritical fluid has drawn many attentions from researchers. Experimental studies have been carried out investigating the in-tube heat transfer characteristics of supercritical fluids (e.g. water

* Corresponding author.
*E-mail address:* y.li.1@bham.ac.uk (Y. Li).

https://doi.org/10.1016/j.ijthermalsci.2022.108001
Received 6 December 2020; Received in revised form 21 October 2022; Accepted 25 October 2022
Available online 7 November 2022

and $CO_2$) [10,14,17], correlations have been built to characterize the internal flow heat transfer behaviors of supercritical fluids [20–22] and numerical simulations have been conducted also to further understand internal flow heat transfer of supercritical fluids [9,24–26].

In terms of the type of supercritical fluid, the focus on supercritical $N_2$ internal flow heat transfer has not been as much as on supercritical $CO_2$ [2,3,14–16,25,26] and water [10–13,21,24]. One possible reason might be supercritical $N_2$ is usually in much lower temperatures (e.g. ~ −147 °C), which is experimentally and practically more difficult to be dealt with. However, the lack of studies in internal flow convective heat transfer of supercritical $N_2$ does not conform to the current trend of supercritical $N_2$ becoming to play more important roles as a promising cryogenic heat transfer fluid in applications such as liquid air liquefaction and superconducting transition [18,23]. Only limited number of studies about supercritical $N_2$ internal flow convective heat transfer can be found in the literature. Dimitrov et al. [17] experimentally evaluated forced convective heat transfer to supercritical $N_2$ in a vertical circular tube with various mass flow rates, inlet temperatures and heat fluxes. It was pointed out that the heat transfer coefficient (HTC) of $N_2$ first increased and then hit a maximum peak before starting to decrease to the end of the test section. Zhang et al. [18] both experimentally and numerically investigated the flow and heat transfer behaviors of supercritical $N_2$ in a small vertical circular tube at different heat flux, mass flux and inlet fluid temperature conditions. It was suggested that the local HTC of $N_2$ was considerably dependent on the effects of thermo-physical property variation and buoyancy force, while the impact of flow acceleration could be neglected. It was also shown that the Dittus-Boelter correlation [27] and Yoon correlation [28] failed to predict the experimental $N_2$ heat transfer data mainly due to the lack of considering the buoyancy effect. Tatsumoto et al. [19] looked into the forced convection heat transfer of subcooled liquid $N_2$ in a heated vertical tube through experiments. It was claimed that a newly proposed Nusselt number correlation obtained by modifying the Dittus-Boelter correlation could correlate the experimental data of not only non-cryogenic supercritical fluids like water and $CO_2$ but also cryogenic supercritical fluids like helium and nitrogen. Negoescu et al. [9] numerically studied the convective heat transfer of supercritical $N_2$ flowing vertically in a circular tube at a series of mass flux, heat flux and pressure conditions. A remarkable HTC peak was observed near the fluid's pseudo-critical point at a system pressure (3.5 MPa) closer to the supercritical pressure of $N_2$ (3.4 MPa), but not at a pressure further away (7 MPa) since the $N_2$ thermo-physical properties vary much less significant without outstanding peak values for properties like specific heat and thermal conductivity.

Furthermore, as it may be known, having well-established correlations is essential to a new heat transfer study, no matter experimental or numerical, because the correlations can be used as references for comparison to validate new data and also guide relevant discussions to reveal the true mechanisms behind physical phenomena. Correlations have been developed for in-tube convective heat transfer of supercritical fluids, originated either from the Dittus-Boelter correlation [27] or Gnielinski's correlation [38,39]. The Dittus-Boelter correlation is defined as follows,

$$Nu = \frac{h \bullet d}{k} = 0.023 \bullet Re^{0.8} \bullet Pr^{0.4} \tag{1}$$

where $h$, $d$, $Nu$, $k$, $Re$, Pr are convective heat transfer coefficient, tube inner diameter, Nusselt number, fluid thermal conductivity, Reynolds number and Prandtl number of the fluid, respectively.

The Gnielinski correlation is defined as follows,

$$Nu = \frac{(\xi_0/8) \bullet Re \bullet Pr}{1.07 + 12.7 \bullet \sqrt{\xi_0/8} \bullet \left(Pr^{2/3} - 1\right)}$$

$$\xi_0 = [1.82 \bullet \log_{10}(Re) - 1.64]^{-2} \tag{2}$$

Tables A1 and A2 selectively summarize the most representative correlations for supercritical fluids in-tube heat transfer under the form of Dittus-Boelter correlation and Gnielinski's correlation, respectively. As shown in the tables, most of the correlations keep the basic formats of either Dittus-Boelter or Gnielinski's correlation but with a variety of modifications to further account for the additional effects from thermo-physical property variations and buoyancy force as the fluid temperature increases over pseudo-critical temperature. For instance, the temperature difference between the fluid near the heated wall and the bulk fluid core as well as the corresponding thermo-physical property differences have been taken into account by introducing wall-to-bulk ratios such as $\frac{\overline{c_p}}{c_{p_b}}$, $\frac{\rho_w}{\rho_b}$, $\frac{\mu_w}{\mu_b}$, $\frac{k_w}{k_b}$ to the basic forms of correlations [31,33,41–43]. Furthermore, there have been a few studies addressing the heat transfer of supercritical fluids separately in individual heat transfer regions based on the fluid phase conditions along the heated tube considering the thermo-physical properties significantly vary before, at and after the pseudo-critical points. Yamagata et al. [10] split the whole heat transfer process of supercritical water into three regions, fluid temperature lower, very close to and higher than the pseudo-critical temperature. Bae and Kim [34] broke the entire in-channel convective heat transfer process of supercritical $CO_2$ according to the evolution of buoyancy effect by tracking the buoyancy number (Bu). Individual correlations were constructed respectively for different buoyancy number ranges and levels of buoyancy effects. However, despite of the fact that the number of available correlations is greater under the form of Dittus-Boelter correlation than the Gnielinski's correlation, the two groups of correlations are inherently similar. Both groups of correlations express the internal flow convective heat transfer of supercritical fluids in the forms of Reynolds number and Prandtl number considering momentum as well as energy diffusions. Nevertheless, by examining Tables A1 and A2, not even a single group of two correlations were built under the same operating conditions (i.e. type of fluid, pressure, mass flux, heat flux) and therefore, theoretically, it should not be expected that those correlations would be able to fit the heat transfer data well from another research work under different testing conditions [33,37,40]. Based on the literature review, the ultimate generalization of heat transfer correlation for supercritical fluid flowing in channel may not be achievable since each supercritical fluid has its own thermo-physical properties and operating ranges differing from other supercritical fluids. Therefore, it is reasonable and necessary to consider developing exclusive heat transfer correlation for individual supercritical fluid on a case by case basis. It can also be observed from the tables that all the correlations are either for supercritical $CO_2$ or water. Indeed, very few correlations can be found in the literature that was solely created for internal flow convective heat transfer of supercritical $N_2$, especially in small tubes (diameter <10 mm). As a result, Negoescu et al. [9], Zhang et al. [18], and Wang et al. [23] who previously studied on supercritical $N_2$ heat transfer in small tubes had to compare their results with the Dittus-Boelter correlation which was originally developed for single phase flows at subcritical conditions and correlations developed for supercritical $CO_2$ and water. Until very recently, Cheng et al. [47] proposed a heat transfer correlation based on the experimental data of supercritical nitrogen in a heated vertical tube but with relatively large diameter (20 mm).

Overall, supercritical nitrogen is an alternative cryogenic fluid which has promising potentials in e.g. cold energy recovery and storage [9] and superconducting transition [18]. However, the amount of available studies on supercritical nitrogen heat transfer is quite limited. The database of supercritical nitrogen heat transfer is far from complete and needs to be complemented by more empirical data and correlations. Therefore, it is very instructive to conduct further investigation on internal flow heat transfer of supercritical nitrogen. In this study, internal flow convective heat transfer experiments were carried out with $N_2$ transforming from subcritical to supercritical conditions and flowing upwardly in a uniformly heated small circular bare stainless steel tube

(4.57 mm ID). The diameter was selected for investigation based on relevant studies about supercritical fluids in literature, which is within the range of typical tube diameter in supercritical fluid power cycle applications [10,14,18]. The heat transfer experiments were carried out under a series of experimental conditions including pressures at 3.5, 4 MPa, mass fluxes of 27.9, 38.1, 50.8 kg/m$^2$-s and heat fluxes of 8.1, 9.3, 11.2 kW/m$^2$. The mass fluxes were chosen to ensure fluid flows in turbulence regime. The heat fluxes were picked to restrict $N_2$ conditions within the interested subcritical-to-supercritical heat transfer range. The two pressures were selected with one closer to the supercritical pressure of $N_2$ (3.4 MPa) and one further away for comparison, considering the thermo-physical properties of $N_2$ vary more dramatic at a pressure near its supercritical pressure. More specifically, Fig. 1 shows the thermo-physical properties of $N_2$ as a function of temperature at the pressures of 3.5 and 4 MPa above its critical pressure of 3.4 MPa. It can be noticed from the figures that the thermo-physical properties of $N_2$ experience significant variations when changing from subcritical to supercritical conditions. At a certain temperature point, the specific heat and thermal conductivity of $N_2$ have maximum peaks. That point corresponds to the maximum peak value of specific heat is called the fluid's pseudo-critical point. As also shown in Fig. 1, the pseudo-critical temperature is lower and the thermo-physical property variations are more extraordinary at 3.5 MPa than 4 MPa as 3.5 MPa is closer to the critical pressure of $N_2$ at 3.4 MPa. In present study, after the heat transfer characteristics of supercritical $N_2$ was validated and comprehensively interpreted, a new group of heat transfer correlations was proposed for near-supercritical $N_2$ flowing upwardly through a heated vertical circular plain tube.

## 2. . Experimental set-up

### 2.1. Experimental apparatus

The convective heat transfer experiments of supercritical $N_2$ in present study were carried out using experimental apparatus shown in Fig. 2. Pressurized gas $N_2$ was supplied to the system from two parallel gas cylinders. The flow rate of $N_2$ was controlled by a pressure regulator while the flow rate reading was given by a flow meter sitting downstream of the system. The system pressure was regulated using a pressure controller. A heat exchange coil chilled in a liquid nitrogen thermostatic bath (−196 °C) was used to condense $N_2$ from gas to liquid phase. The liquid phase $N_2$ would enter a vertical oriented test tube and

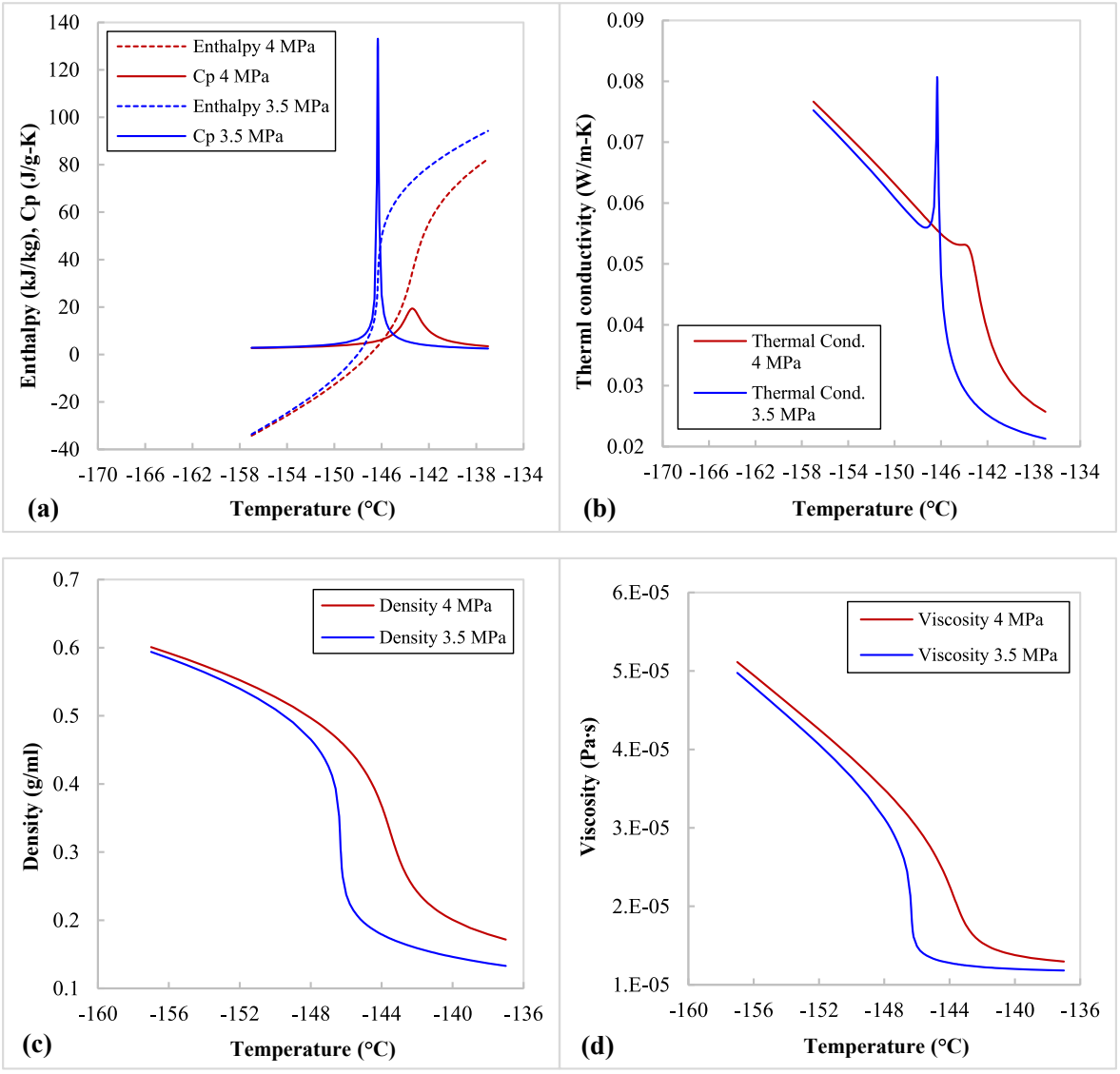


**Fig. 1.** Nitrogen properties below and beyond pseudo-critical points at supercritical pressures 3.5 and 4 MPa, respectively: (a) specific enthalpy and specific heat; (b) thermal conductivity; (c) density; (d) viscosity.

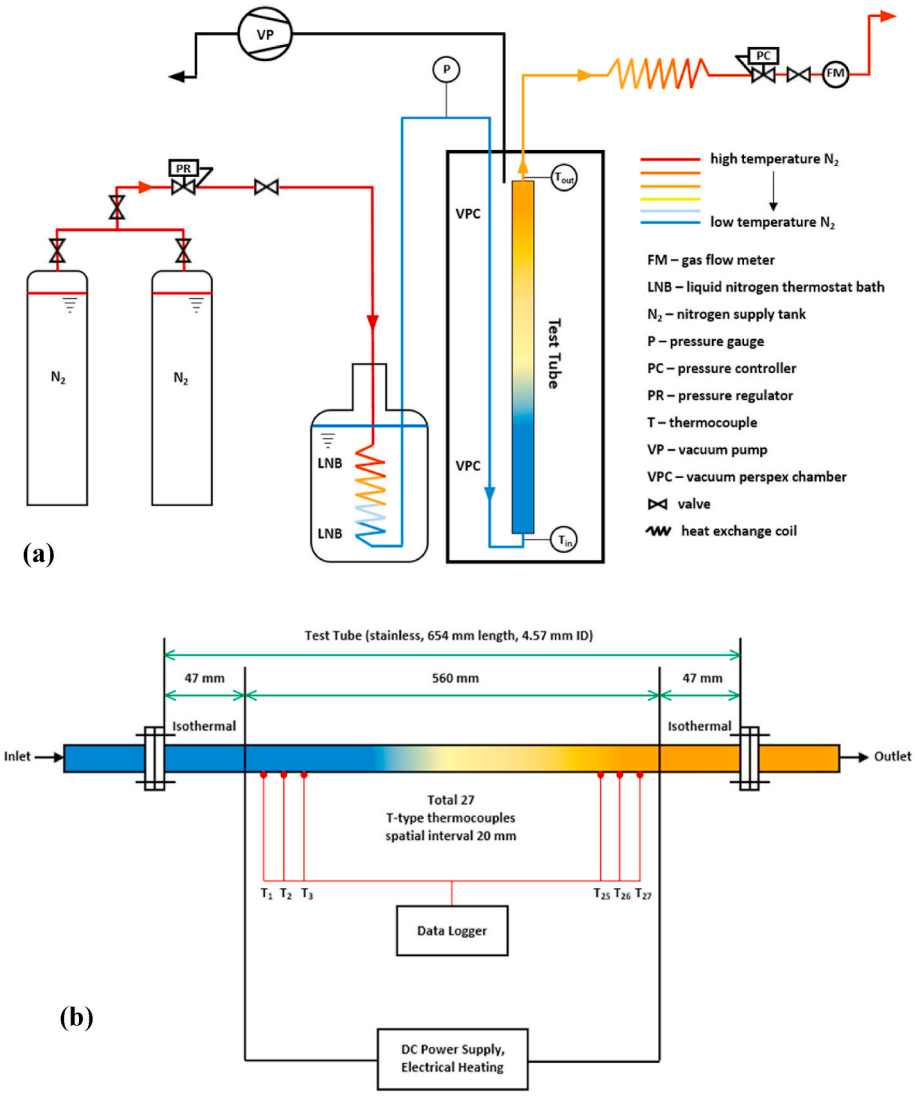


**Fig. 2.** (a) System schematic of supercritical nitrogen in-tube heat transfer experiments (b) Heat transfer test tube.

be heated under constant heat flux conditions when flowing past the tube. The test tube was placed in a vacuum perspex chamber to prevent heat losses. Two Type T thermocouples were installed to measure the inlet and outlet temperatures of the working fluid. The fluid temperature difference between the inlet and outlet of the test section was deliberately managed to thoroughly cover the interested pseudo-critical transition and thermo-physical property variation region of the tested $N_2$.

The heat transfer test tube is further demonstrated in Fig. 2 (b). It has an inner diameter of 4.57 and outer diameter of 6.35 mm, respectively. A direct current power supply was used to provide electrical heating to the test tube. The constant heat flux condition was ensured for 560 mm of the tube. 27 T-type thermocouples (20 mm interval each) were evenly spread along the 560 mm test section to measure the axial wall temperature distribution of the heated stainless steel tube under convective cooling. All thermocouples in the experimental system were connected to a Graphtec data logger for real-time data acquisition. Moreover, isothermal conditions were applied to a 47 mm of the test tube length after the inlet and 47 mm before the outlet. More details about the experimental system and heat transfer test section can be found in a previous study [23].

### 2.2. Experimental uncertainties and data reduction

In internal flow heat transfer, heat transfer coefficient (HTC) quantifies the convective heat transfer rate between a heated tube wall and the heat transfer fluid. The HTC of supercritical $N_2$ undergoing pseudo-critical transition and flowing through the heated test tube is defined as follows:

$$h = \frac{q''}{(T_w - T_b)} \tag{3}$$

where q'', $T_w$, and $T_b$ are the supplied heat flux at tube wall, tube inner wall temperature, and bulk fluid temperature, respectively. Notice local tube outer temperatures were measured through surface mounted thermocouples during experiments and $T_w$ the tube inner wall temperature can be approximately calculated using the 1-D heat conduction equation,

$$q'' = k \bullet \frac{(T_w - T_{outer})}{(\Delta x)} \tag{4}$$

where k, $T_{outer}$ and $\Delta x$ are the thermal conductivity of tube material (13 W/m-K for stainless steel 316), tube outer wall temperature directly measured by thermocouples and tube wall thickness (0.89 mm), respectively.

The actual heat flux values used in Eq. (3) for data reduction always took into account the heat losses of the experimental system, which was approximately 7% of the total input power, though the heat transfer test tube was placed in vacuum to prevent heat losses. The system heat loss was determined through power calibration experiments by comparing the actual input power from power supply and the enthalpy difference of test fluid between at the inlet and outlet of the test tube. The enthalpy difference was experimentally aquired based on the measured inlet and outlet fluid temperatures and $N_2$ thermo-physical properties from the National Institute of Standards and Technology (NIST) database. The local fluid temperature $T_b$ was obtained by looking up NIST $N_2$ property table based on local $N_2$ enthalpy, which was calculated as follows:

$$H_{local} = H_{in} + 4 \bullet \frac{q''}{G} \bullet \frac{x}{d} \tag{5}$$

where $H_{local}$, $H_{in}$, $G$, $x$, $d$ are the local fluid enthalpy, fluid inlet enthalpy, fluid mass flux, axial location along the test tube length and the tube inner diameter, respectively.

Furthermore, the sensors used for experimental measurements and their associated uncertainties were specified in Table 1. All the sensors were calibrated before the heat transfer experiments. For example, thermocouple readings were calibrated under both isothermal and heating/cooling temperature condtions. Thermocouple calibration equations were applied to each thermocouple reading for more accurate results. The uncertainty analysis of experimental results, mainly HTC values), was conducted following the multivariate propagation of error approach, as shown below in Eq. (6). The final experimental uncertainty values were reflected against HTC values of supercritical $N_2$, indicated as error bars in Figs. 3–10 under the results section.

$$\sigma_U = \sqrt{\left(\frac{\partial U}{\partial X_1}\right)^2 \sigma_{X_1}^2 + \left(\frac{\partial U}{\partial X_2}\right)^2 \sigma_{X_2}^2 + \ldots + \left(\frac{\partial U}{\partial X_n}\right)^2 \sigma_{X_n}^2} \tag{6}$$

where: $U$: given function of independent variables, $U = U(X_1, X_2, \ldots, X_n)$ $X_n$: independent variable $\sigma_{Xn}$: uncertainty associated with corresponding independent variable, $X_n$ $\sigma_U$: uncertainty associated with dependent variable $U$.

**Table 1**
Measured variables, instruments and the associated uncertainties.

| Measured Parameters | Uncertainties | Instruments | Specifications (Accuracies) |
|---|---|---|---|
| Pressure | ±0.005 MPa | Alicat scientific pressure measuring and controller, PCH-100 PSIA | ±0.125% of read value |
| Power | ±1 W | Elektro-Automatik Analogue, digital bench power supply, EA-PS 9080-120-2U | <0.1% of read value<br><0.002 V<br><0.08 A |
| T | ±0.5 °C | Thermon Ltd., type-T thermocouple | ±0.5 °C |
| Flow rate | ±0.3 L/min | Omega, FMA-A2323 digital flowmeter | ±1% of full scale<br>±0.3 SLM |
| L | ±1 mm | SS316 stainless steel tube | ±1 mm of length |
| d | ±0.1 mm | SS316 stainless steel tube | ±0.1 mm of diameter |

## 3. Results and discussion

### 3.1. The effects of pressure, heat flux and mass flux on heat transfer of $N_2$ transforming from subcritical to supercritical in a vertical tube

Researchers have tried to understand internal flow convective heat transfer of supercritical fluids, mainly water and $CO_2$, through the effects of pressure, heat flux and mass flux [9,11,14,18]. Thus, similarly in this study, the effects of pressure, heat flux and mass flux on the convective heat transfer characteristics of $N_2$ transiting across the pseudo-critical point in a heated vertical small plain tube were experimentally explored. The HTC results under conditions of different pressures (3.5, 4 MPa), mass fluxes (27.9, 38.1, 50.8 kg/m$^2$-s) and heat fluxes (8.1, 9.3, 11.2 kW/m$^2$) are plotted against fluid specific enthalpy in Figs. 3–6, respectively. As the figures show, the HTCs of $N_2$ first increased to a peak maximum and then significantly decreased with the fluid specific enthalpy for all considered experimental conditions, which follows the typical HTC trend of supercritical fluids near their pseudo-critical points [10,14,17]. The decrease in HTC for supercritical fluids is mainly due to the variations in fluid thermo-physical properties and the aggravated effect of buoyancy as distinct phase difference no longer exists and supercritical fluid behaves more like vapor at temperatures above pseudo-critical temperature [15,18,44].

Moreover, it can be found in Figs. 3 and 4 that, under a same heat

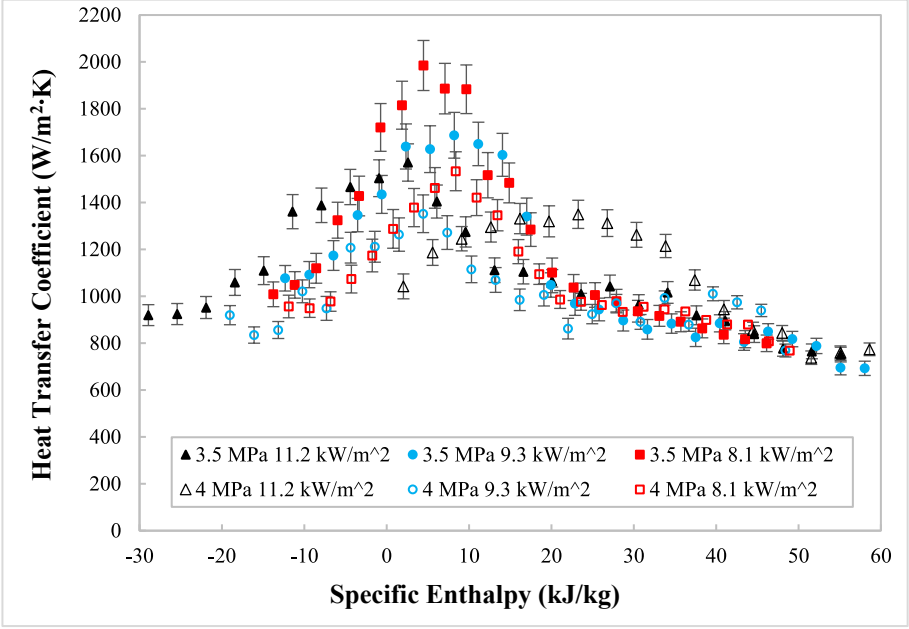


**Fig. 3.** Heat transfer coefficients as a function of local $N_2$ enthalpy at mass flux of 50.8 kg/m$^2$-s for different pressures and heat fluxes.

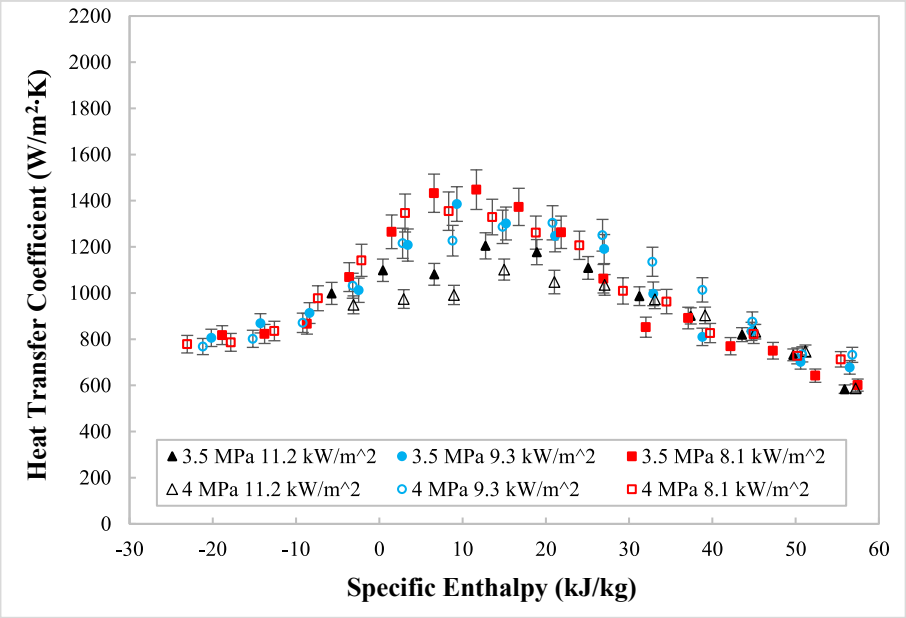


**Fig. 4.** Heat transfer coefficients as a function of local $N_2$ enthalpy at mass flux of 27.9 kg/m$^2$-s for different pressures and heat fluxes.

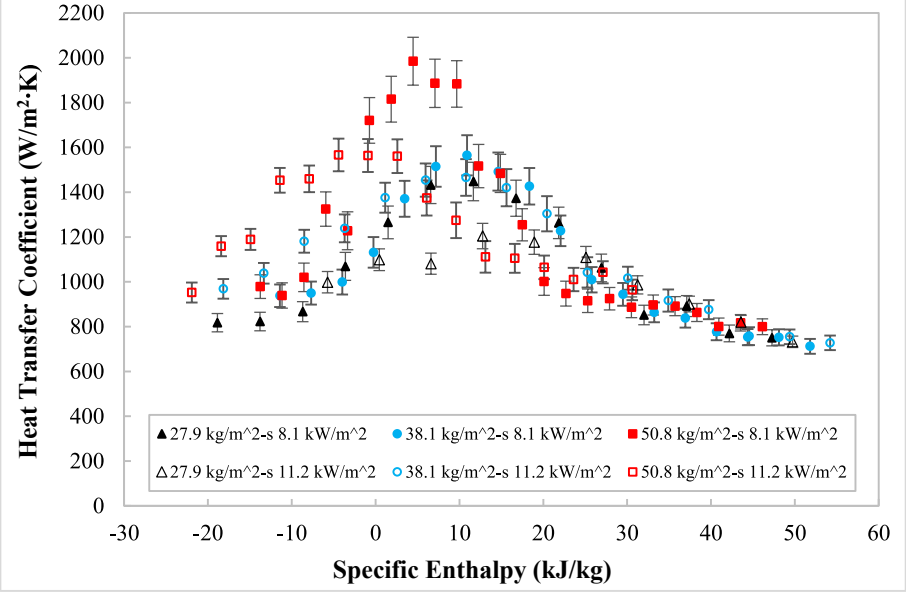


**Fig. 5.** Heat transfer coefficients as a function of local $N_2$ enthalpy at 3.5 MPa pressure for different mass fluxes and heat fluxes.

flux and mass flux (e.g. 9.3 kW/m$^2$ and 50.8 kg/m$^2$-s or 8.1 kW/m$^2$ and 27.9 kg/m$^2$-s), the HTC values are greater for the cases at 3.5 MPa pressure than 4 MPa, especially for the peak HTC values. Such result is consistent with other supercritical fluid studies [9,10,14]. The main explanation for this pressure-related phenomenon is the differences in $N_2$ thermo-physical properties between 3.5 and 4 MPa as illustrated earlier in Fig. 1. The heat transfer characteristics of $N_2$ near pseudo-critical point, i.e. Reynolds and Prandtl number, are governed by corresponding $N_2$ thermo-physical properties. The specific heat and thermal conductivity of $N_2$ are greater at 3.5 MPa than 4 MPa featuring a better thermal transport potential at 3.5 MPa. Also, $N_2$ has a smaller viscosity at 3.5 MPa, which leads to a higher Reynolds number and thereby intensified turbulence for cases at 3.5 MPa when both 3.5 MPa and 4 MPa cases are under the same tube diameter and mass flux. The intensified turbulent benefits convective heat transfer of $N_2$ and is another reason for higher HTCs at 3.5 MPa than 4 MPa.

In addition, as indicated in Figs. 3 and 4, at a given mass flux and pressure (e.g. 3.5 MPa and 50.8 kg/m$^2$-s or 4 MPa and 27.9 kg/m$^2$-s), the HTC values increased as heat flux decreased (i.e. from 11.2 to 9.3 to 8.1 kW/m$^2$), which has also been observed in similar supercritical fluid studies [9,10,14]. This might be because the tube wall temperature is higher at higher heat fluxes leading to higher fluid temperatures near the tube wall (above pseudo-critical temperature). The supercritical fluid would behave more like vapor with lower thermal conductivity, specific heat, density and viscosity as its temperature continues to increase above pseudo-critical temperature, which would result in exacerbated buoyancy effect and deteriorated heat transfer. In addition, as it can be seen in Fig. 1, the specific heat and thermal conductivity values of $N_2$ significantly increase near its pseudo-critical point, which is desired for better heat transfer. However, the temporal and spatial effects of

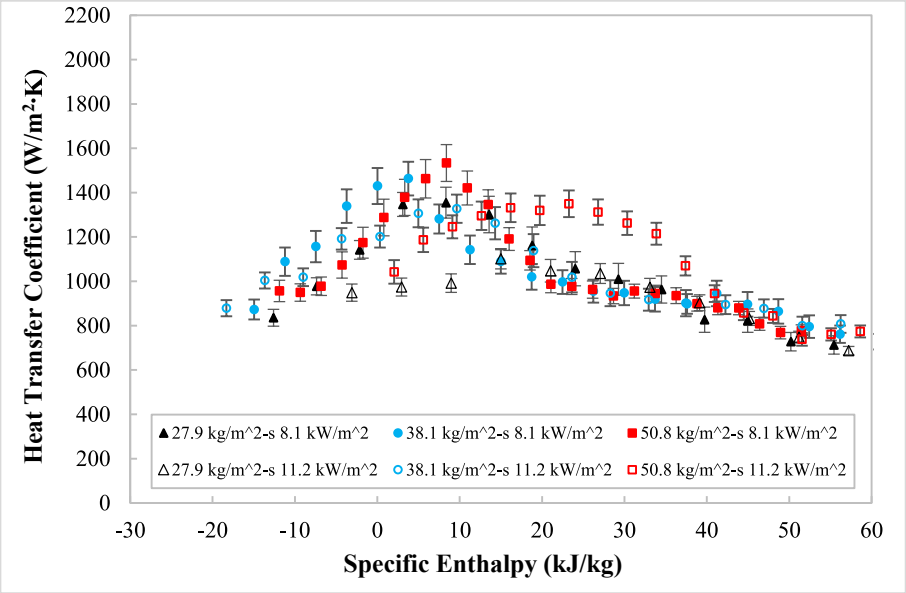


**Fig. 6.** Heat transfer coefficients as a function of local $N_2$ enthalpy at 4 MPa pressure for different mass fluxes and heat fluxes.

those peak specific heat and thermal conductivity value regions on heat transfer are attenuated (i.e. disappear quicker) under high heat fluxes as supercritical $N_2$ develops towards temperatures greater than pseudo-critical temperature more rapidly.

On the other hand, the effect of mass flux on convective heat transfer of supercritical $N_2$ is relatively straightforward. For example, under 3.5 MPa and 8.1 kW/m$^2$ in Fig. 5 4 MPa and 11.2 kW/m$^2$ in Fig. 6, the heat transfer performance and HTC values of $N_2$ get enhanced as mass flux increases. The rise in mass flux accelerates the fluid and improves turbulence in the tube leading to superior convective heat transfer and greater HTC values.

### 3.2. *Comparison between experimental results and predictions from established correlations*

Though it has been demonstrated in Section 3.1 that the experimental internal flow heat transfer results of supercritical $N_2$ in present study obey the general trend of supercritical fluids and are consistent with the major findings in other similar studies, it is still necessary to further validate the obtained experimental data. Unfortunately, there are very few research work regarding internal flow convective heat transfer of supercritical $N_2$ available in the literature let alone heat transfer correlations exclusively developed for supercritical $N_2$ despite of the fact that investigations on supercritical water and $CO_2$ are ubiquitous. The missing of similar studies and corresponding heat transfer correlations cause difficulties in comparing, validating and understanding experimental results for studies like present study and will continue for future studies on this topic. As a result, the experimental results of internal flow convective HTCs of supercritical $N_2$ in present study had to be compared and validated with heat transfer correlations for supercritical water and $CO_2$ under different experimental conditions as listed in Tables A1 and A2.

The comparisons among experimental HTC results of supercritical $N_2$ and correlated HTC values are displayed in Figs. 7 and 8. As the figures indicate, most of the HTC correlations for single phase fluid and supercritical water and $CO_2$ failed to describe the HTC results of supercritical $N_2$. Specifically, the Dittus-Boelter correlation [27] overestimated the experimental HTC values and shifted the HTC vs. specific enthalpy curve to the right. Consistently, the Dittus-Boelter correlation was found to overestimate the HTC values of supercritical water and $CO_2$ also [9,14,35,45]. Hence, usually suppression factors have to be introduced to the Dittus-Boelter correlation when developing the HTC correlations for supercritical water and $CO_2$, which can be seen from Tables A1 and A2. However, most of the HTC correlations for supercritical water and $CO_2$ underestimate the HTC values for supercritical $N_2$ as shown in Figs. 7 and 8, suggesting the suppression factors of Dittus-Boelter correlations for supercritical water and $CO_2$ cannot be equivalently transplanted to supercritical $N_2$ (i.e. the correlated HTC values get over-suppressed). Moreover, the correlations that underestimate the experimental HTC values of supercritical $N_2$ shift the HTC vs. specific enthalpy curve either to the left or right of the experimental values. Thus, it can be noticed that most of the HTC correlations for supercritical water and $CO_2$ fall short in fitting the HTC values for supercritical $N_2$ mainly due to the differences in fluid thermo-physical properties and experimental conditions among supercritical water, $CO_2$ and $N_2$. Nevertheless, the correlated HTC values from Yamagata correlation [10], which was proposed for supercritical water, most closely matched with the experimental HTC values of supercritical $N_2$ in present study, as demonstrated in Figs. 7 and 8. The most important reason for this success might be that the internal flow convective heat transfer of supercritical fluid was divided into different regions in Yamagata correlation using Eckert number as the determining criteria, as shown in Table A1. The Eckert number is one of the most important measures for the phase condition of a fluid passing through a heated tube cross section, defined as follows:

$$E = \frac{(T_c - T_b)}{(T_w - T_b)} \tag{7}$$

where $T_c$ is the fluid critical temperature at a given pressure. Based on the definition in Equation (7), if the Eckert number is greater than 1, the

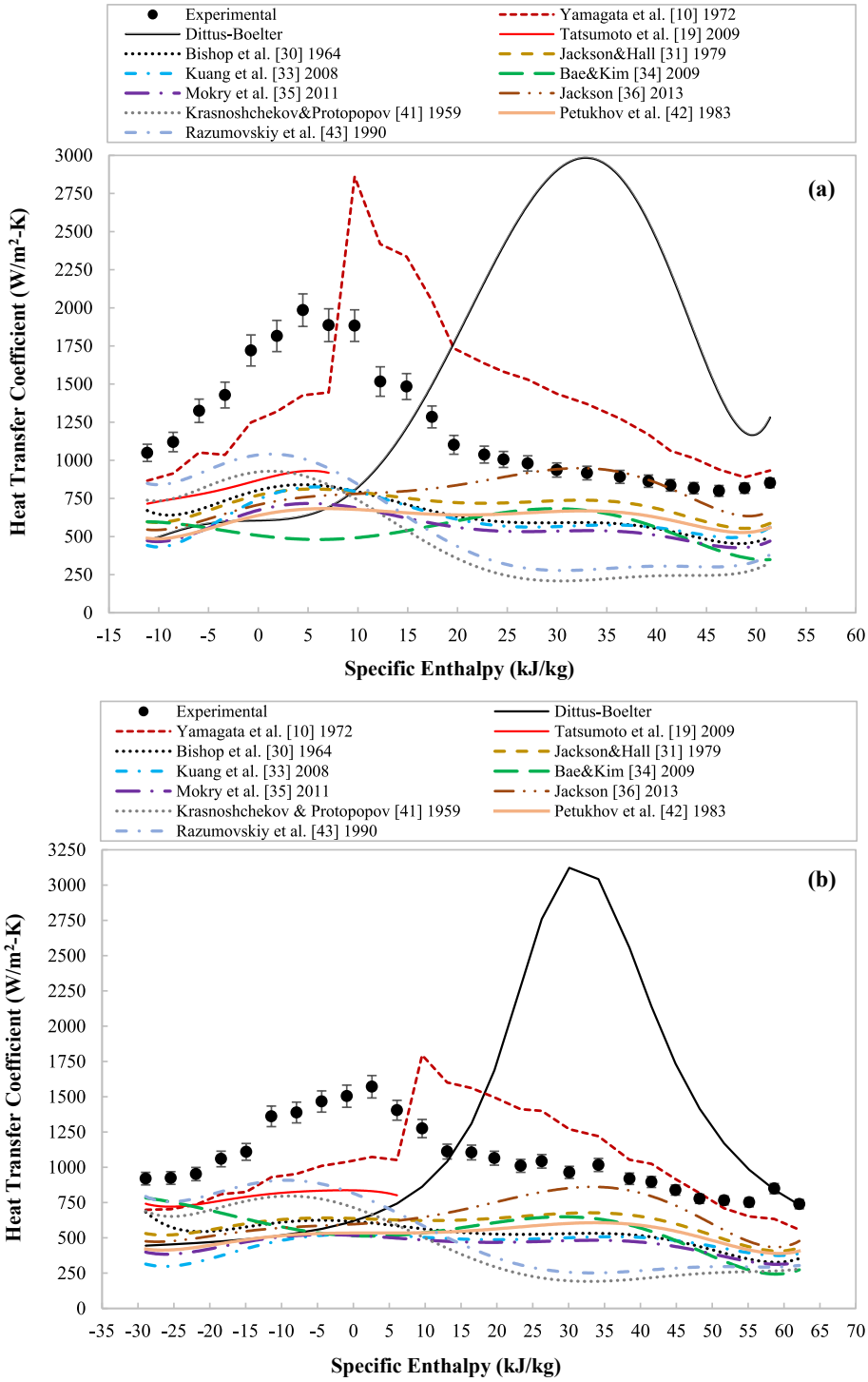


**Fig. 7.** Comparisons among experimental HTC results and correlated HTC values at conditions of (a) 3.5 MPa, 50.8 kg/m$^2$-s, 8.1 kW/m$^2$ (b) 3.5 MPa, 50.8 kg/m$^2$-s, 11.2 kW/m$^2$.

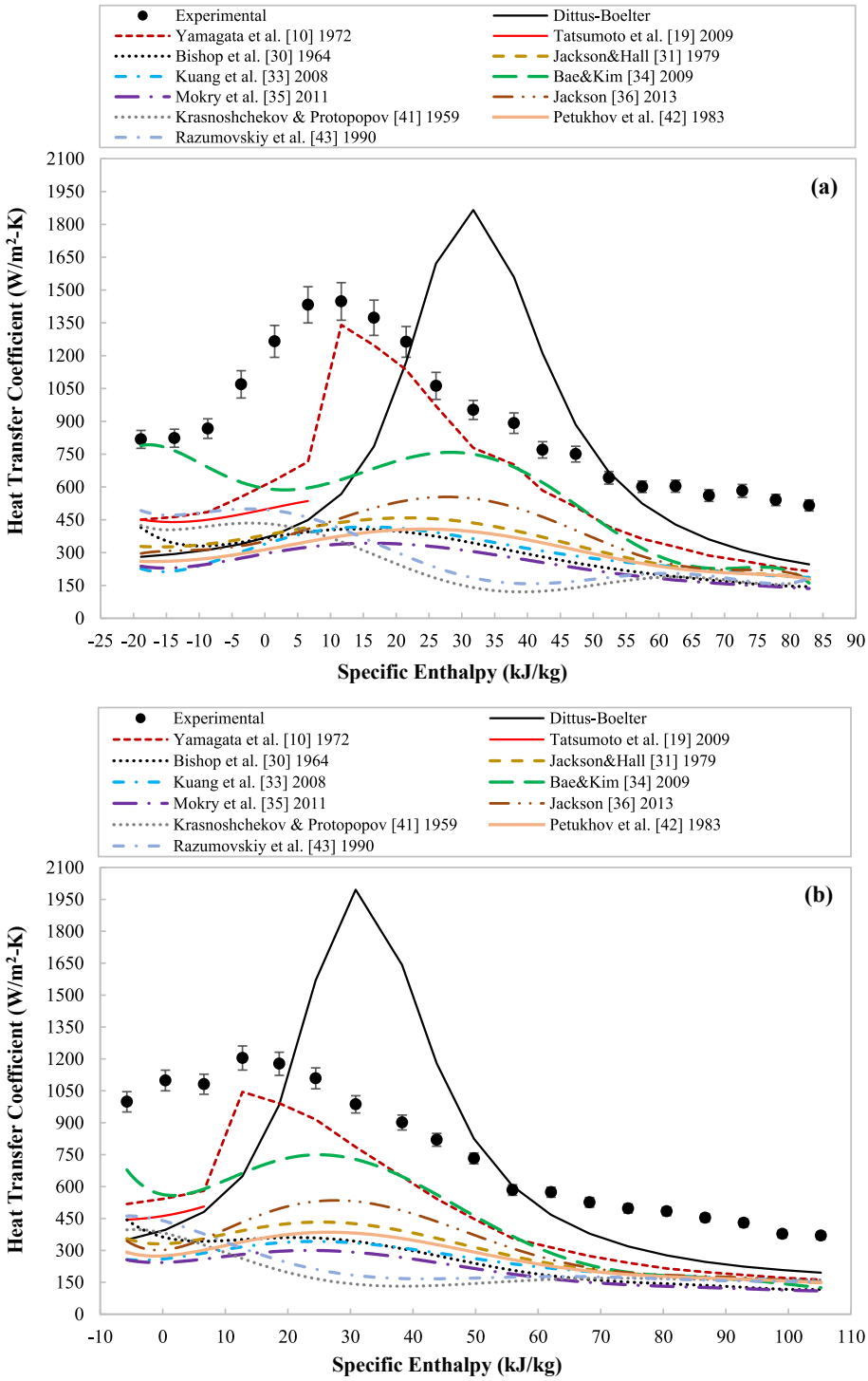


**Fig. 8.** Comparisons among experimental HTC results and correlated HTC values at conditions of (a) 3.5 MPa, 27.9 kg/m$^2$-s, 8.1 kW/m$^2$ (b) 3.5 MPa, 27.9 kg/m$^2$-s, 11.2 kW/m$^2$.

fluid is in liquid phase, while is in vapor/supercritical phase if $E < 0$. The fluid is near its pseudo-critical condition when $0 \leq E \leq 1$.

### *3.3. Construction of a new heat transfer correlation for $N_2$ transforming from subcritical to supercritical in a heated vertical tube*

Based on the existing heat transfer correlations for supercritical water and $CO_2$ in Tables A1 and A2 and the fact that most of those correlations fell short in predicting the experimental heat transfer data of supercritical $N_2$ as shown in Figs. 7 and 8, a new correlation exclusively for $N_2$ is demanded to better characterize the internal flow convective heat transfer behaviors of supercritical $N_2$ in the vicinity of its pseudo-critical point. Similar to the heat transfer correlations for supercritical water and $CO_2$, a new heat transfer correlation for $N_2$ was constructed not only in the form of Dittus-Boelter equation using Reynolds number and Prandtl number to account for the momentum and energy transports, but also taking into consideration the thermophysical property variations and buoyancy effects, which are the two main features of supercritical $N_2$ in-tube convective heat transfer, by

introducing correction factors such as $\frac{\overline{c_p}}{cp_b}$, $\frac{\rho_w}{\rho_b}$, $\frac{\mu_w}{\mu_b}$, $\frac{k_w}{k_b}$ into the correlation. In this way, both the temperature gradient between heated tube wall and bulk fluid as well as the corresponding effects of fluid thermo-physical property variations and buoyancy on heat transfer performance are addressed in the new correlation. The general form of the newly proposed correlation is as follows:

$$Nu_b = A \bullet Re_b^m \bullet \overline{Pr_b}^n \bullet \left(\frac{\rho_w}{\rho_b}\right)^i \bullet \left(\frac{\mu_w}{\mu_b}\right)^k \bullet \left(\frac{k_w}{k_b}\right)^p \tag{8}$$

where $Nu_b$ is the bulk fluid Nusselt number, $Re_b$ is the bulk fluid Reynolds number, $\overline{Pr_b} = \frac{H_w - H_b}{T_w - T_b} \times \frac{\mu_b}{k_b}$ is an effective Prandtl number taking into account the temperature gradient effect between the heated tube wall and the bulk fluid, $H_w$, $H_b$, $T_w$, $T_b$, $\rho_w$, $\rho_b$, $\mu_w$, $\mu_b$, $k_w$, $k_b$ are the specific enthalpies, temperatures, densities, dynamic viscosities and thermal conductivities of the flowing $N_2$ at the heated tube wall and the bulk fluid core, respectively.

Equation (8) was tested and trained by the experimental data of $N_2$ internal flow convective heat transfer in present study with the empirical coefficients and power indexes in the correlation determined accordingly towards the best fitted values. The relevant experimental data covered three heat flux (i.e. 8.1, 9.3, 11.2 kW/m$^2$) and three mass flux conditions (i.e. 27.9, 38.1, 50.8 kg/m$^2$-s) and were obtained at 3.5 MPa, a pressure condition under which $N_2$ exhibits symbolic thermo-physical property changes across the pseudo-critical point. Furthermore, the entire heat transfer range was categorized to two different regimes according to the Eckert number (Eq. (7)) when Equation (8) was applied [10]. The resulted final form of the proposed convective heat transfer correlation for $N_2$ transiting past the pseudo-critical point in a heated vertical circular tube is as follows:

$$Nu_b = 104.85 \bullet Re_b^{0.26} \bullet \overline{Pr_b}^{-0.083} \bullet \left(\frac{\rho_w}{\rho_b}\right)^{-0.013} \bullet \left(\frac{\mu_w}{\mu_b}\right)^{1.02} \bullet \left(\frac{k_w}{k_b}\right)^{1.39} \quad 0 \le \frac{(T_c - T_b)}{(T_w - T_b)} \le 1.0 \quad 1 < \frac{P}{P_c} < 1.1 \tag{9}$$

$$Nu_b = 124.34 \bullet Re_b^{0.02} \bullet \overline{Pr_b}^{0.16} \bullet \left(\frac{\rho_w}{\rho_b}\right)^{0.63} \bullet \left(\frac{\mu_w}{\mu_b}\right)^{-1.05} \bullet \left(\frac{k_w}{k_b}\right)^{0.75} \frac{(T_c - T_b)}{(T_w - T_b)} \quad < 0 \quad 1 < \frac{P}{P_c} < 1.1 \tag{10}$$

note that nitrogen is in cold liquid phase when E = $\frac{(T_c - T_b)}{(T_w - T_b)}$>1, which is beyond the interested range of this supercritical $N_2$ study.

### 3.4. Validation of the new supercritical $N_2$ heat transfer correlation

To demonstrate the capabilities of the newly developed correlation in characterizing the internal flow convective heat transfer behaviors of $N_2$ before, near and after its pseudo-critical point, the correlated HTC values from the proposed correlation together with other selected correlations in Table A1 and A2 are plotted against the corresponding experimental HTC values. Not all correlations from Tables A1 and A2 were picked, but those were found to more accurately fit with each experimental data set, as shown and discussed in Figs. 7 and 8. The comparisons between correlated HTC values and experimental values are illustrated in Fig. 9 for high and Fig. 10 for low mass flux at three heat fluxes, respectively. As it can be noticed, the HTC values obtained from the newly proposed correlation best matched with the experimental values within minimal errors for both HTC and fluid specific enthalpy results, outperforming all the other correlations. Furthermore, it is shown in Figs. 9–11 that the newly proposed correlation is more than capable of correlating the experimental heat transfer data of supercritical $N_2$ within approximately 10% and at least 15% considering all the experimental data acquired at pressure 3.5 MPa.

The competitiveness of the newly developed correlation in terms of predicting the in-tube convective heat transfer characteristics of supercritical $N_2$ were further demonstrated by evaluating the mean absolute percentage error (MAPE) and root mean squared percentage error (RMSPE) between the correlated HTC values and the experimental values, defined as follows:

$$\text{MAPE} = \frac{1}{N}\sum_{i=1}^{N}\left|\frac{Experimental_i - Correlated_i}{Experimental_i}\right| \tag{11}$$

$$\text{RMSPE} = \sqrt{\frac{1}{N}\sum_{i=1}^{N}\left(\frac{Experimental_i - Correlated_i}{Experimental_i}\right)^2} \tag{12}$$

As indicated in Tables 2 and 3, the newly proposed correlation, which was tailored exclusively for supercritical $N_2$, is the most outstanding performer in terms of errors against the experimental data with both smallest MAPEs and RMSPEs compared with all the other considered correlations originally developed for supercritical water and $CO_2$.

The newly developed supercritical $N_2$ internal flow convective HTC correlation was examined by comparing with the experimental results of other researchers, from Zhang et al. [18] who conducted similar supercritical $N_2$ experiments (vertical stainless steel tube ID 2 mm) but at another geographic location, time and under different experimental conditions. As it is shown in Figs. 12 and 13, the general trends of experimental HTC values from Zhang et al. [18] were effectively predicted by the HTC correlation proposed in present study for two different heat flux conditions (i.e. 41.3 and 64.2 kW/m$^2$). Furthermore, the correlated HTC values match with individual experimental values in a satisfactory way, approximately within ±35% as indicated in Fig. 12 (b) and Fig. 13 (b). It is worth noting that Zhang et al.'s own numerical simulation results were only able to fit with their experimental HTC data within approximately ±40% error, as presented in Ref. [18], let alone the newly proposed HTC correlation in present study was developed at different experimental conditions from Zhang et al.'s experiments. The proposed HTC correlation was based on experimental results of supercritical $N_2$ flowing upwards and being uniformly heated in 4.57 mm diameter circular tube under 3.5 MPa pressure, 8.1–11.2 kW/m$^2$ heat flux and 27.9–50.8 kg/m$^2$-s mass flux. Instead, the tube diameter, pressure, heat flux and mass flux was 2 mm, 3.6 MPa, 41.3–64.2 kW/m$^2$ and 104–107 kg/m$^2$-s in Zhang et al.'s supercritical $N_2$ experiments. According to the literature, a HTC correlation for supercritical fluids, especially if being applied to predict experimental results obtained at conditions different from which the correlation was originally developed from, would usually produce more than 50% inaccuracy and be seen as fairly worked for within ±50% error [21,34,46]. For further validation, the new correlation was also tested against the experimental data of Tatsumoto et al. [19], in which heat transfer experiments of $N_2$ were conducted in a heated vertical tube (ID 5.4 mm) at 3.5 MPa and for fluid temperatures only lower than pseudo-critical temperature. The validation results are shown in Fig. 14. It can be observed that the new correlation developed in present study is able to predict corresponding experimental data of Tatsumoto et al. [19] within acceptable error range, 19.8% on average.

Although the present study intends to focus on pressure conditions ($1 < \frac{P}{P_c} < 1.1$) close to the critical pressure of $N_2$ (3.4 MPa), which feature the most unique thermophysical property variations and the newly proposed correlation was based on the heat transfer data under 3.5 MPa pressure, to further test the correlation, the correlated HTC values were compared with the experimental values of near pseudocritical and supercritical $N_2$ under 4 MPa pressure as well as HTC values predicted by other correlations, as shown in Figs. 15 and 16. Notice that the thermophysical properties of near pseudocritical $N_2$, including

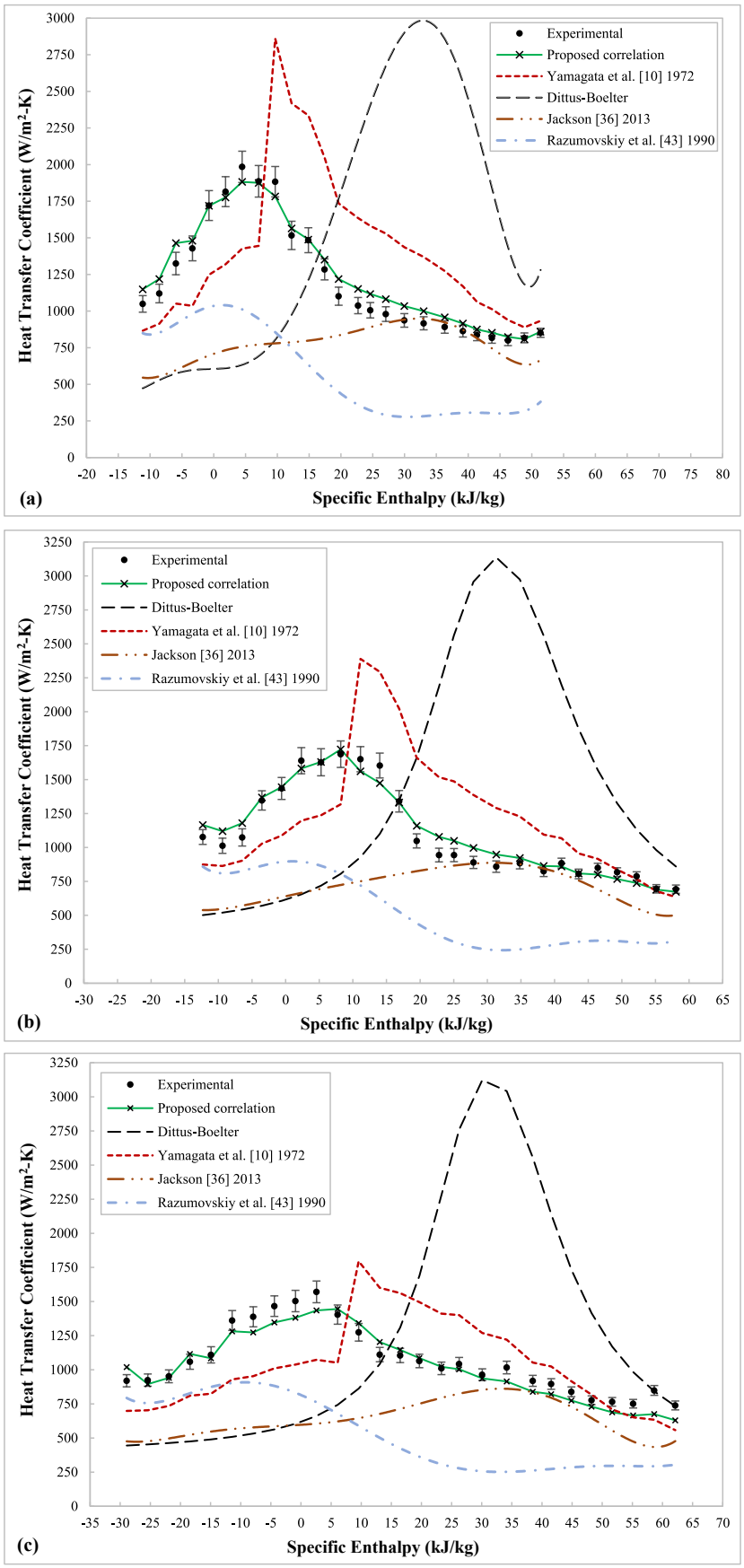


**Fig. 9.** Performance evaluation of the newly proposed HTC correlation in predicting experimental HTC values at conditions of (a) 3.5 MPa, 50.8 kg/m$^2$-s, 8.1 kW/m$^2$ (b) 3.5 MPa, 50.8 kg/m$^2$-s, 9.3 kW/m$^2$ (c) 3.5 MPa, 50.8 kg/m$^2$-s, 11.2 kW/m$^2$.

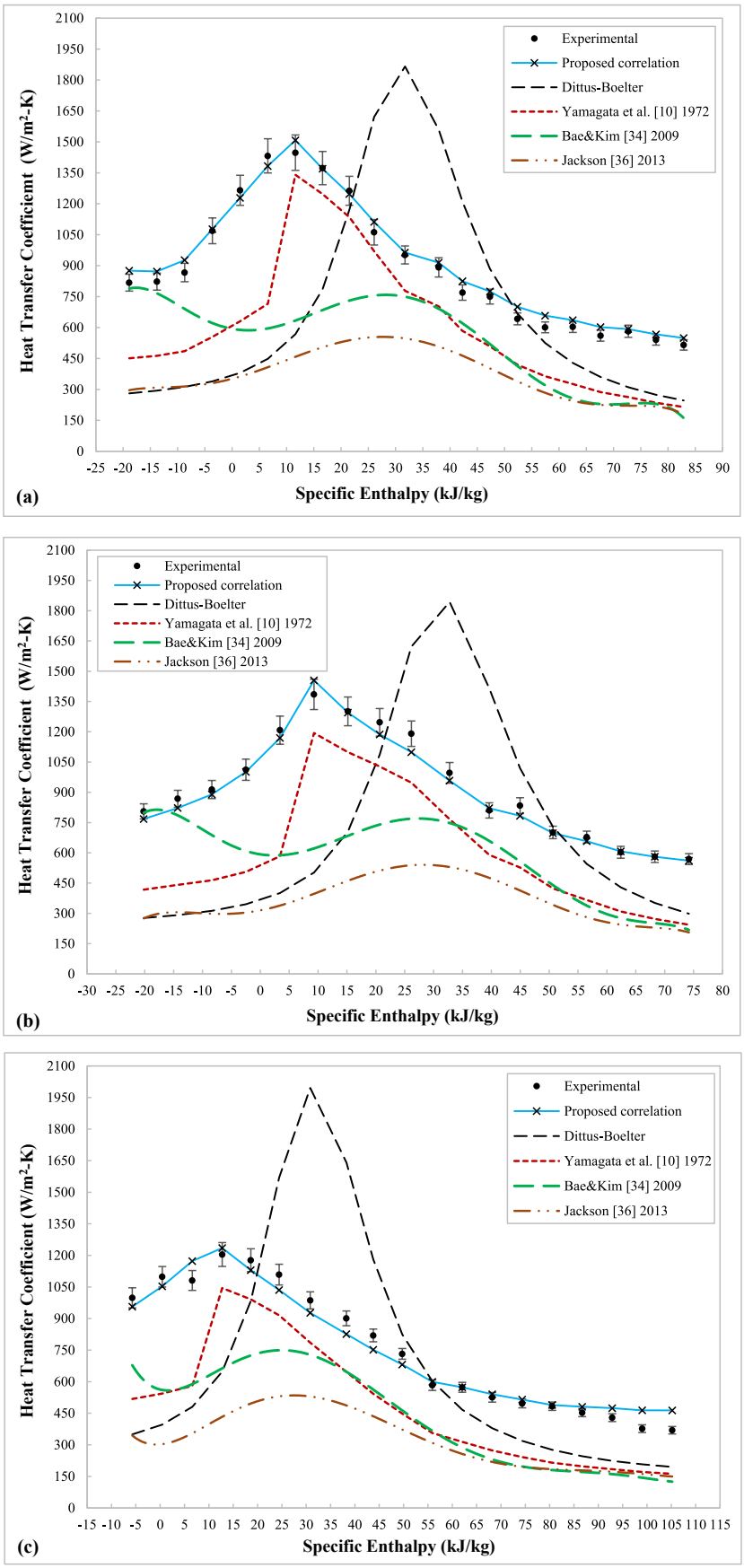


**Fig. 10.** Performance evaluation of the newly proposed HTC correlation in predicting experimental HTC values at conditions of (a) 3.5 MPa, 27.9 kg/m$^2$-s, 8.1 kW/m$^2$ (b) 3.5 MPa, 27.9 kg/m$^2$-s, 9.3 kW/m$^2$ (c) 3.5 MPa, 27.9 kg/m$^2$-s, 11.2 kW/m$^2$.

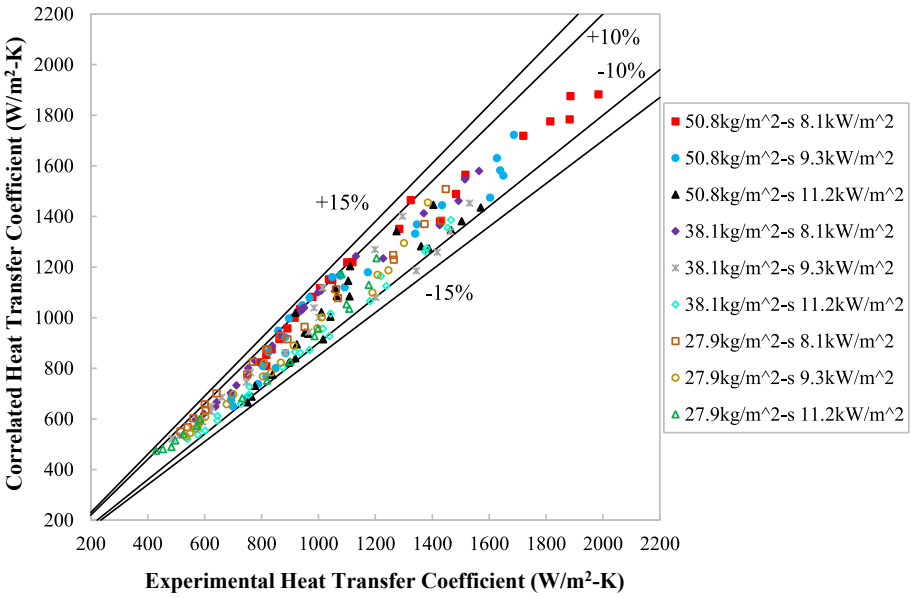


**Fig. 11.** Comparisons among correlated HTC values and experimental HTC values at 3.5 MPa for different mass fluxes and heat fluxes.

**Table 2**
Mean absolute percentage errors (MAPE) for predicting experimental HTC values using correlations including the newly proposed correlation (3.5 MPa pressure).

| MAPE | 27.9 kg/m$^2$-s 8.1 kW/m$^2$ | 27.9 kg/m$^2$-s 9.3 kW/m$^2$ | 27.9 kg/m$^2$-s 11.2 kW/m$^2$ | 50.8 kg/m$^2$-s 8.1 kW/m$^2$ | 50.8 kg/m$^2$-s 9.3 kW/m$^2$ | 50.8 kg/m$^2$-s 11.2 kW/m$^2$ |
|---|---|---|---|---|---|---|
| Proposed Correlation | 4.6% | 2.8% | 7.1% | 6.0% | 5.1% | 6.1% |
| Dittus-Boelter | 46.4% | 45.0% | 41.0% | 93.4% | 85.3% | 79.3% |
| Yamagata [10] 1972 | 33.6% | 38.0% | 38.3% | 39.2% | 27.9% | 25.4% |
| Razumovskiy [43]1990 | – | – | – | 52.6% | 54.2% | 50.2% |
| Bae and Kim [34] 2009 | 40.0% | 40.8% | 44.7% | – | – | – |
| Jackson [36] 2013 | 54.9% | 57.3% | 53.7% | 30.2% | 30.0% | 35.7% |

In bold – the minimum values.

**Table 3**
Root mean squared percentage errors (RMSPE) for predicting experimental HTC values using correlations including the newly proposed correlation (3.5 MPa pressure).

| RMSPE | 27.9 kg/m$^2$-s 8.1 kW/m$^2$ | 27.9 kg/m$^2$-s 9.3 kW/m$^2$ | 27.9 kg/m$^2$-s 11.2 kW/m$^2$ | 50.8 kg/m$^2$-s 8.1 kW/m$^2$ | 50.8 kg/m$^2$-s 9.3 kW/m$^2$ | 50.8 kg/m$^2$-s 11.2 kW/m$^2$ |
|---|---|---|---|---|---|---|
| Proposed Correlation | 5.3% | 3.6% | 9.6% | 7.1% | 6.4% | 6.9% |
| Dittus-Boelter | 52.9% | 51.1% | 47.8% | 114.3% | 114.1% | 98.5% |
| Yamagata [10] 1972 | 38.3% | 42.0% | 41.9% | 44.6% | 33.3% | 28.1% |
| Razumovskiy [43]1990 | – | – | – | 54.9% | 56.5% | 54.4% |
| Bae and Kim [34] 2009 | 44.2% | 44.8% | 47.8% | – | – | – |
| Jackson [36] 2013 | 57.1% | 59.5% | 55.6% | 37.7% | 36.4% | 40.6% |

In bold – the minimum values.

specific heat, thermal conductivity, density and viscosity, are considerably different between under 3.5 MPa and 4 MPa pressures, as shown in Fig. 1. It can be seen from Figs. 15 and 16 that the newly developed correlation overpredicts the HTC values near the pseudocritical point due to the considerable thermophysical property differences between near pseudocritical $N_2$ at 3.5 MPa and 4 MPa pressures. But the correlated HTC values start to match well with the experimental HTC values as $N_2$ fluid temperature increases over its pseudocritical temperature as the differences in thermophsycial properties between at 3.5 MPa and 4 MPa pressures diminish (see Fig. 1). Furthermore, the results in Figs. 15 and 16 indicate that the newly developed correlation, though is intended to be mainly used for pressure range of $1 < \frac{P}{P_c} < 1.1$, still outperforms most of the other correlations in terms of predicting the experimental HTC values of $N_2$ being heated over its pseudocritical point via convective heat transfer in a straight tube with small diameters. In addition, the HTC values predicted by the newly proposed correlation are plotted against the experimental HTC values under 4 MPa pressure in Fig. 17. The figure provides further interpretation to the results in Figs. 15 and 16, as most correlated HTC values fall within 30% error, some are between 30% and 40% error and only a few beyond 40% error against the experimental HTC values.

## 4. Conclusions

In this study, convective heat transfer experiments of $N_2$ transforming from subcritical to supercritical near its pseudo-critical point were carried out as $N_2$ flowing upwardly in a heated vertical circular bare stainless steel tube (ID 4.57 mm) under experimental conditions including pressures of 3.5, 4.0 MPa, fluid mass fluxes of 27.9, 38.1, 50.8 kg/m$^2$-s and constant heat fluxes of 8.1, 9.3, 11.2 kW/m$^2$, respectively. The main purpose of this work is to investigate the unique characteristics of near pseudocritical $N_2$ internal flow convective heat transfer, construct a suitable heat transfer correlation exclusively for supercritical $N_2$ under pressures close to its critical pressure, thereby complementing the database of supercritical $N_2$ heat transfer and create a useful reference for future related studies. The primary concluding remarks based on the experimental results are as follows:

- The heat transfer of $N_2$ undergoing pseudo-critical transition and flowing upwardly in a heated circular plain tube followed the general heat transfer trend found in other supercritical fluids such as water

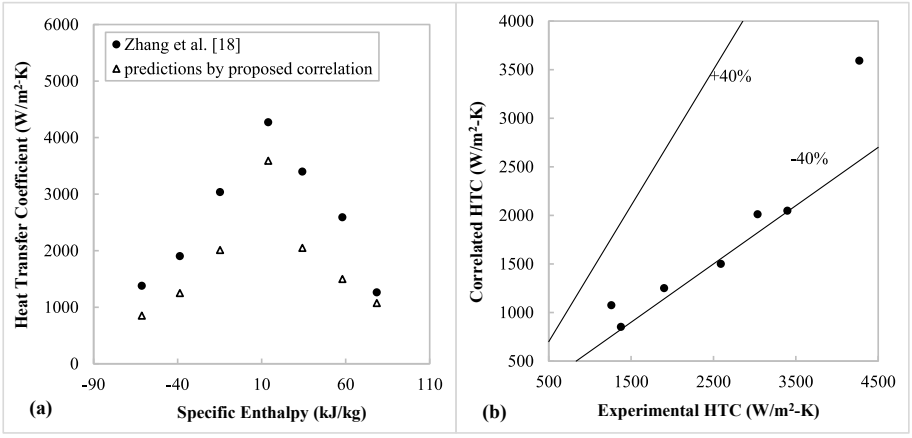


**Fig. 12.** Comparison between predicted HTC values via the newly proposed correlation and experimental HTC results from Zhang et al. [18] in a 2 mm ID circular tube under 3.6 MPa, 105.5 kg/m$^2$-s and 41.3 kW/m$^2$.

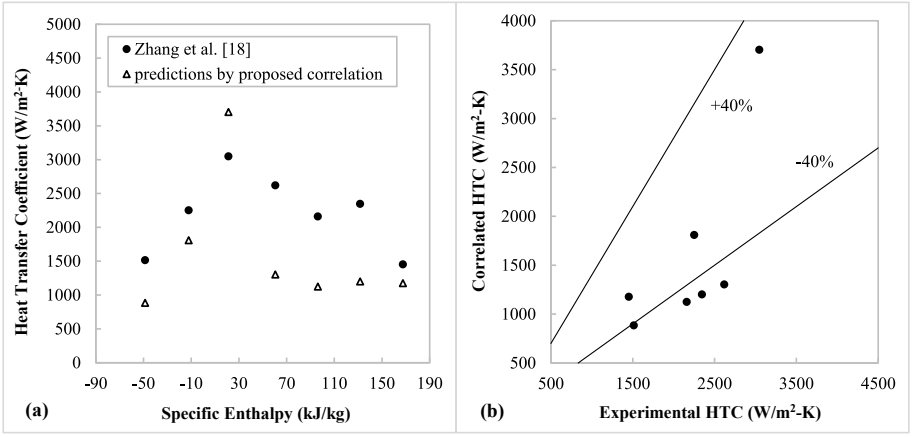


**Fig. 13.** Comparison between predicted HTC values via the newly proposed correlation and experimental HTC results from Zhang et al. [18] in a 2 mm ID circular tube under 3.6 MPa, 105.5 kg/m$^2$-s and 64.2 kW/m$^2$.

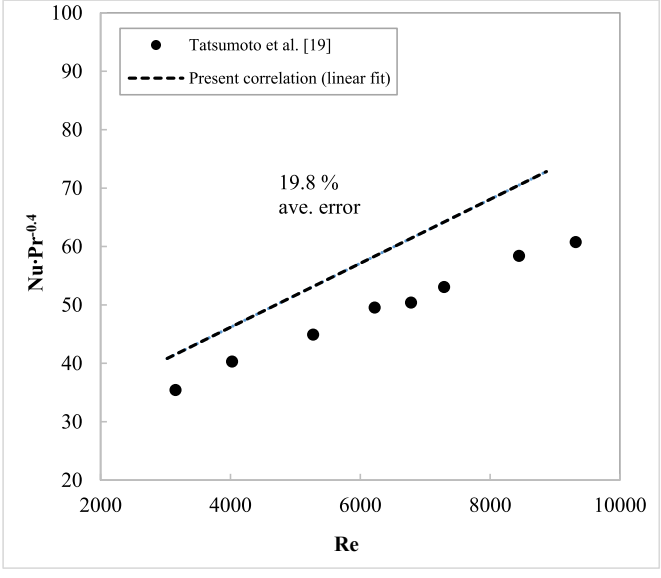


**Fig. 14.** Comparison between predicted heat transfer results via the newly proposed correlation and experimental data from Tatsumoto et al. [19] in a 5.4 mm ID stainless steel circular tube under 3.5 MPa.

and $CO_2$, with the convective heat transfer coefficient first rising to a maximum peak value near the pseudo-critical point and then continuously deteriorating as the supercritical fluid temperature becomes higher than pseudo-critical temperature.

- Local heat transfer coefficient values of $N_2$ increased with fluid mass flux due to enhanced turbulence but decreased with pressure and heat flux, which significantly affect the thermo-physical properties of $N_2$. The thermo-physical property variations and associated buoyancy effects dominate the heat transfer behavior of $N_2$ in the vicinity of pseudo-critical point (i.e. the appearance of heat transfer coefficient peak, the heat transfer coefficient increase before and deteriorate after the heat transfer coefficient peak).
- The Dittus-Boelter correlation, which is more suitable for single phase flows and heat transfer correlations originally developed for supercritical water and $CO_2$ under experimental conditions that were different from those in present study were unable to predict the heat transfer coefficient values for $N_2$.
- A new heat transfer correlation has been proposed exclusively aiming to characterize the internal flow convective heat transfer of $N_2$ transforming from subcritical to supercritical conditions under pressures close to its critical pressure and flowing upwardly in a heated small circular bare tube. The new correlation inherited the basic form of Dittus-Boelter correlation, but took additional considerations of fluid thermo-physical property differences between the heated wall and bulk fluid core and employed Eckert number to

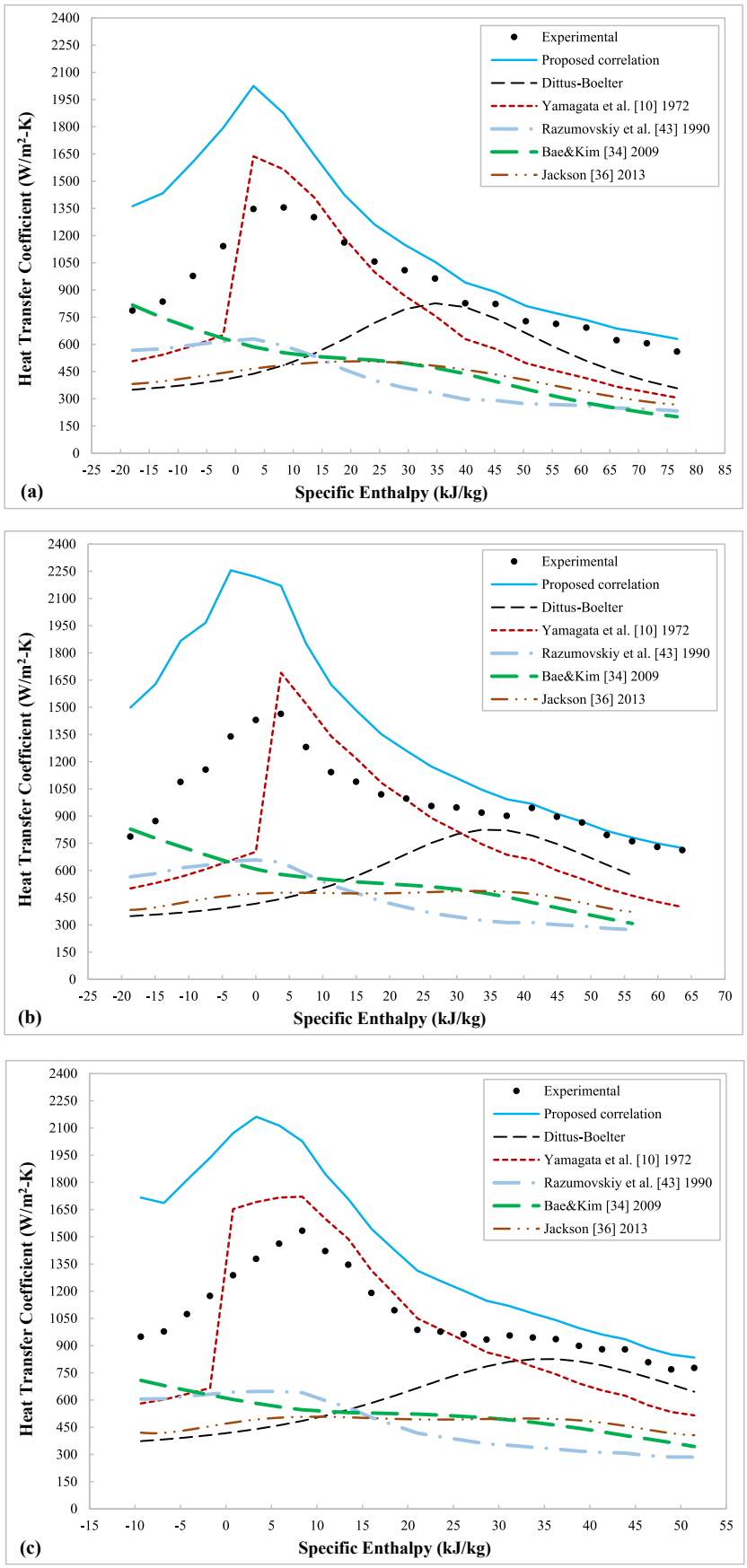


**Fig. 15.** Performance evaluation of the newly proposed HTC correlation in predicting experimental HTC values under 4 MPa at conditions of (a) 27.9 kg/m$^2$-s, 8.1 kW/m$^2$ (b) 38.1 kg/m$^2$-s, 8.1 kW/m$^2$ (c) 50.8 kg/m$^2$-s, 8.1 kW/m$^2$.

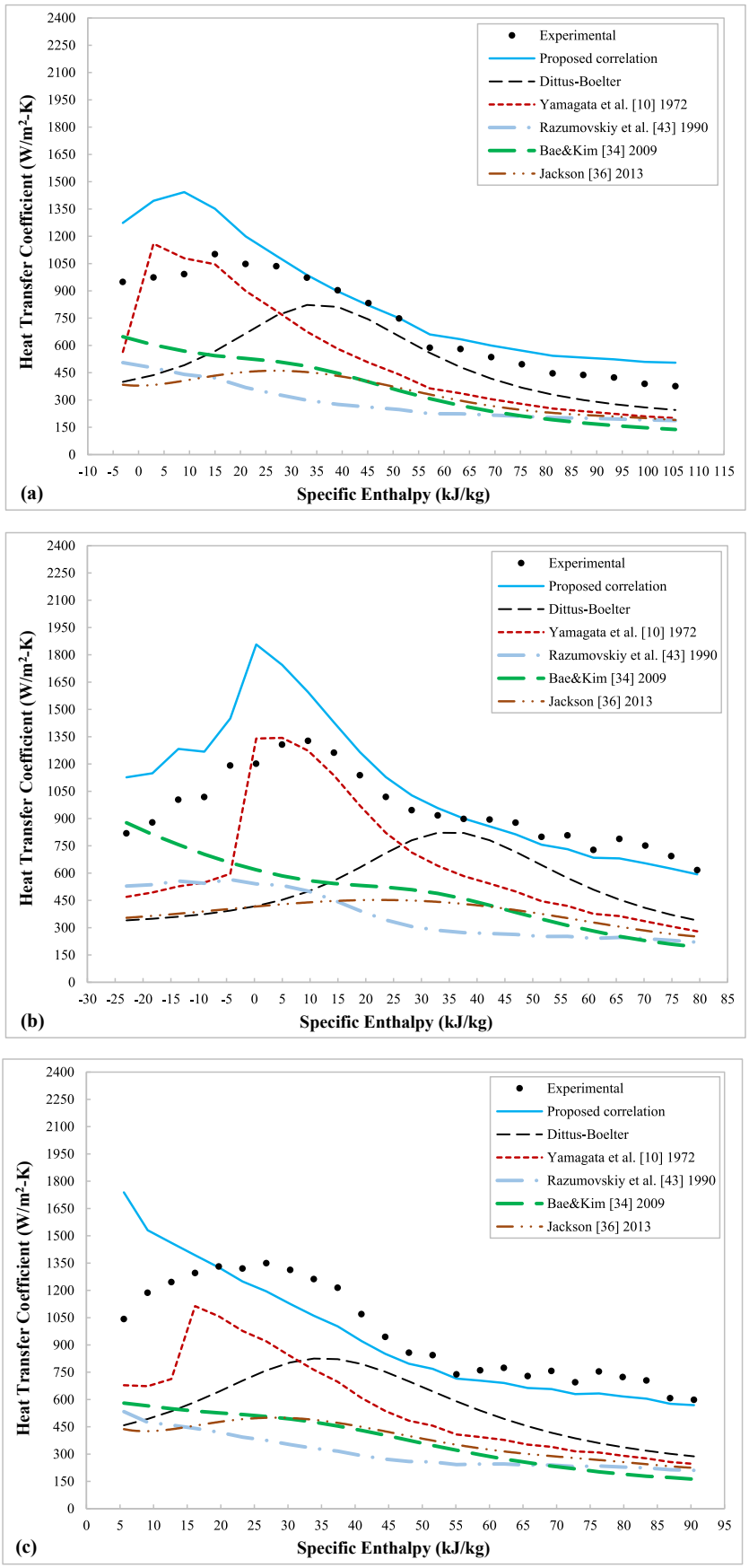


**Fig. 16.** Performance evaluation of the newly proposed HTC correlation in predicting experimental HTC values under 4 MPa at conditions of (a) 27.9 kg/m$^2$-s, 11.2 kW/m$^2$ (b) 38.1 kg/m$^2$-s, 11.2 kW/m$^2$ (c) 50.8 kg/m$^2$-s, 11.2 kW/m$^2$.

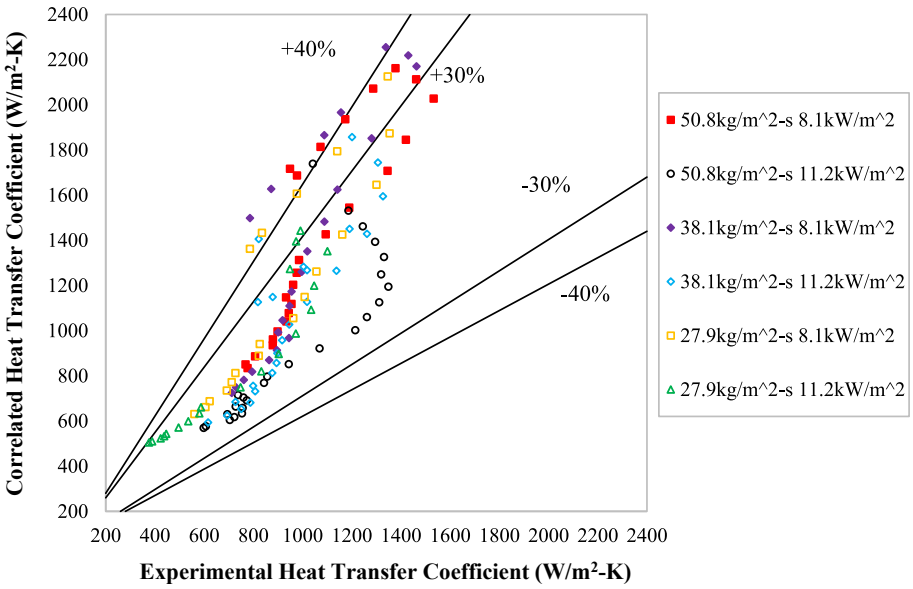


**Fig. 17.** Comparisons among correlated HTC values and experimental HTC values at 4 MPa for different mass fluxes and heat fluxes.

categorize the whole heat transfer process into three regions around the pseudo-critical point.

- The newly developed heat transfer correlation demonstrated superior competence in correlating with the experimental results of present study, approximately within ±10% errors. The applicability of the newly developed heat transfer correlation was also examined by correlating with experimental results from other studies on convective heat transfer of supercritical $N_2$ under pressures close to its critical pressure. The correlated HTC values from the heat transfer correlation were matched well with the experimental HTC values from Zhang et al. [18] within approximately ±35% and Tatsumoto et al. [19] within approximately ±20%, respectively, even though the heat transfer correlation was developed under different experimental conditions from those in Zhang et al.'s and Tatsumoto et al.'s study.

Overall, the reach of one research study is limited and the heat transfer correlation developed in present study focuses on conditions close to the critical pressure of $N_2$ ($1 < \frac{P}{P_c} < 1.1$), in which near-pseudocritical $N_2$ has the most unique thermal properties. The results also suggest heat transfer correlations should be developed separately for supercritical $N_2$ close to and away from its critical pressure, when near the pseudocritical points. Therefore, although the proposed heat transfer correlations could be a stepping stone to provide guidance for future studies, the work to complete the database of supercritical $N_2$ internal flow convective heat transfer is far from accomplished. More experiments as well as numerical simulations are needed to cover more supercritical $N_2$ conditions for more accurate heat transfer correlations that are applicable to wider ranges.

## Declaration of competing interest

The authors declare that they have no known competing financial interests or personal relationships that could have appeared to influence the work reported in this paper.

## Data availability

Data will be made available on request.

## Acknowledgement

The authors would like to acknowledge the financial support of the Engineering and Physical Sciences Research Council (EPSRC) of the United Kingdom (Grant Nos.EP/N000714/1 and EP/N021142/1). The project has also received funding from the European Union's Horizon 2020 research and innovation programme under the Marie Sklodowska-Curie grant agreement No. 101007976.

## Appendix

**Table A1**
Important correlations for supercritical fluids internal flow heat transfer in the form of Dittus-Boelter correlation [27].

| Author | Fluid | Correlation | Operating Condition |
|---|---|---|---|
| Bishop et al., 1964 [30] | water | $Nu_b = 0.0069 \bullet Re_b^{0.9} \bullet \overline{Pr_b}^{0.66} \bullet \left(\frac{\rho_w}{\rho_b}\right)^{0.43} \bullet \left(1 + 2.4 \bullet \frac{d}{x}\right)$<br>$\overline{Pr_b} = \frac{H_w - H_b}{T_w - T_b} \times \frac{\mu_b}{k_b}$ | d: 2.5, 5.1 mm,<br>P: 22.6–27.5 MPa<br>G: 0.68–3.6 ton/m$^2$•s,<br>q'': 0.31–3.5 MW/m$^2$<br>Flow orientation: ↑ |
| Swenson et al., 1965 [29] | water | $Nu_w = 0.0459 \bullet Re_w^{0.923} \bullet \left(\overline{c_p} \bullet \frac{\mu_w}{k_w}\right)^{0.613} \bullet \left(\frac{\rho_w}{\rho_b}\right)^{0.231}$<br>$\overline{c_p} = \frac{H_w - H_b}{T_w - T_b}$ | d: 9.4 mm,<br>P: 22.7–41.3 MPa<br>G: 0.2–2.0 ton/m$^2$-s,<br>q'': 0.2–2.0 MW/m$^2$<br>Flow orientation: ↑ |
| Yamagata et al., 1972 [10] | water | | d: 7.5, 10 mm, |

(*continued on next page*)

**Table A1** (*continued*)

| Author | Fluid | Correlation | Operating Condition |
|---|---|---|---|
| | | $Nu_b = 0.0135 \bullet Re_b^{0.85} \bullet Pr_b^{0.8} \bullet F_c$<br>$F_c = \begin{cases} 1.0 & (t_{pc}-t_b)/(t_w-t_b) > 1.0 \\ 0.67 \bullet Pr_{pc}^{-0.05} \bullet \left(\frac{\overline{c_p}}{cp_b}\right)^{n1} & 0 \le (t_{pc}-t_b)/(t_w-t_b) \le 1.0 \\ \left(\frac{\overline{c_p}}{cp_b}\right)^{n2} & (t_{pc}-t_b)/(t_w-t_b) < 0 \end{cases}$<br>$n1 = -0.77 \bullet \left(1+\frac{1}{Pr_{pc}}\right) + 1.49;\ n2 = 1.44 \bullet \left(1+\frac{1}{Pr_{pc}}\right) - 0.53$ | P: 22.6–29.4 MPa<br>G: 0.31–1.83 ton/m$^2$•s,<br>q'': 0.12–0.93 MW/m$^2$<br>Flow orientation:<br>→, ↑, ↓ |
| Jackson and Hall 1979 [31] | $CO_2$ | $Nu_b = 0.0183 \bullet Re_b^{0.82} \bullet \overline{Pr_b}^{0.5} \bullet \left(\frac{\rho_w}{\rho_b}\right)^{0.3}$<br>$\overline{Pr_b} = \frac{H_w - H_b}{T_w - T_b} \times \frac{\mu_b}{k_b}$ | d: 4.08 mm,<br>P: 7.85, 9.81 MPa<br>G: 0.35 ton/m$^2$•s,<br>q'': <2.6 MW/m$^2$<br>Flow orientation: ↑ |
| Gorban and Pometko 1990 [32] | Water R-12 | $Nu_b = 0.0059 \bullet Re_b^{0.9} \bullet Pr_b^{-0.12}$ | $T_b > T_{cr}$<br>Flow orientation: ↑ |
| Kuang et al., 2008 [33] | water | $Nu_b = 0.024 \bullet Re_b^{0.76} \bullet \overline{Pr_b}^{0.83} \bullet \left(\frac{\rho_w}{\rho_b}\right)^{0.31} \bullet \left(\frac{\mu_w}{\mu_b}\right)^{0.83} \bullet \left(\frac{k_w}{k_b}\right)^{0.086} \bullet (Gr^*)^{0.014} \bullet (q^+)^{-0.021}$<br>$Gr^* = \frac{g \bullet \beta \bullet D^4 \bullet q}{k \bullet \nu^2}$<br>$q^+ = \frac{q \bullet \beta}{G \bullet c_p}$<br>$\overline{Pr_b} = \frac{H_w - H_b}{T_w - T_b} \times \frac{\mu_b}{k_b}$ | P: 22.75–31.03 MPa<br>G: 0.35–3.6 ton/m$^2$•s,<br>q'': 0.23–3.47 MW/m$^2$<br>Flow orientation: ↑ |
| Bae and Kim 2009 [34] | $CO_2$ | $Nu_b = Nu_v \bullet f(Bu)$<br>$Nu_v = 0.021 \bullet Re_b^{0.82} \bullet Pr_b^{0.5} \bullet \left(\frac{\rho_w}{\rho_b}\right)^{0.3} \bullet \left(\frac{\overline{c_p}}{cp_b}\right)^{n}$<br>For details of $f(Bu)$, please refer to [34] | d: 6.32 mm,<br>P: 7.75–8.55 MPa<br>G: < 1.2 ton/m$^2$•s,<br>q'': <0.15 MW/m$^2$<br>Flow orientation: ↑ |
| Mokry et al., 2011 [35] | water | $Nu_b = 0.0061 \bullet Re_b^{0.914} \bullet \overline{Pr_b}^{0.654} \bullet \left(\frac{\rho_w}{\rho_b}\right)^{0.518}$<br>$\overline{Pr_b} = \frac{H_w - H_b}{T_w - T_b} \times \frac{\mu_b}{k_b}$ | d: 3–38 mm,<br>P: 22.8–29.4 MPa<br>G: 0.2–1.5 ton/m$^2$•s,<br>q'': <1.25 MW/m$^2$<br>Flow orientation: ↑ |
| Jackson 2013 [36] | $CO_2$ | $Nu_b = 0.0183 \bullet Re_b^{0.82} \bullet Pr_b^{0.5} \bullet \left(\frac{\rho_w}{\rho_b}\right)^{0.3} \bullet \left(\frac{\overline{c_p}}{cp_b}\right)^{n}$<br>For details of index n, please refer to [36] | d: 4.1 mm,<br>P: 7.8–9.8 MPa<br>Re: 8•10$^4$–5•10$^5$,<br>q'': <0.26 MW/m$^2$<br>Flow orientation: ↑ |
| Deev et al., 2018 [37] | water | $Nu_b = 0.023 \bullet Re_b^{0.8} \bullet Pr_b^{0.4} \bullet \left(\frac{\rho_w}{\rho_b}\right)^{0.25} \bullet \left(\frac{\overline{c_p}}{cp_b}\right)^{n} \bullet Y$<br>$Y = (1-\xi) \bullet Y_1 + \xi \bullet Y_2$<br>$Y_1 = 1 + a_1 \bullet exp(b_1 K_h^2 + c_1 K_h)$<br>$Y_2 = 1 + a_2 \bullet exp(b_2 K_h^2 + c_2 K_h)$<br>$\xi = exp(-0.5 \bullet (K_{Am})^2)$, weight coefficient in expression for $Y$<br>$K_h = K_{Am} \bullet (H_b - H_{pc})/H_{pc}$ | d: 2.67–12.0 mm,<br>P: 22.6–26 MPa<br>G: < 2 ton/m$^2$•s,<br>q'': 0.2–2.25 MW/m$^2$<br>Flow orientation: ↑ |

**Table A2**
Representative correlations for supercritical fluids internal flow heat transfer in the form of Gnielinski correlation [38,39].

| Author | Fluid | Correlation | Operating Condition |
|---|---|---|---|
| Krasnoshchekov and Protopopov 1959 [41] | Water $CO_2$ | $Nu_b = Nu_0 \bullet \left(\frac{\mu_w}{\mu_b}\right)^{0.11} \bullet \left(\frac{k_w}{k_b}\right)^{0.33} \bullet \left(\frac{\overline{c_p}}{cp_b}\right)^{0.35}$<br>$Nu_0 = \frac{(\xi_0/8) \bullet Re_b \bullet \overline{Pr_b}}{1.07 + 12.7 \bullet \sqrt{\xi_0/8} \bullet (\overline{Pr_b}^{2/3} - 1)}$<br>$\xi_0 = [1.82 \bullet \log_{10}(Re_b) - 1.64]^{-2}$ | P: 22.3–32 MPa (water);<br>8.3 MPa ($CO_2$),<br>Re: 2•10$^4$–8.6•10$^5$<br>Flow orientation: ↑ |
| Petukhov et al., 1983 [42] | $CO_2$ | $Nu_b = \frac{(\xi/8) \bullet Re_b \bullet \overline{Pr_b}}{1 + 900/Re_b + 12.7 \bullet \sqrt{\xi/8} \bullet (\overline{Pr_b}^{2/3} - 1)}$<br>$\xi = \xi_0 \bullet \left(\frac{\mu_w}{\mu_b}\right)^{0.2} \bullet \left(\frac{\rho_w}{\rho_b}\right)^{0.4}$ | d: 8 mm,<br>P: 7.7, 8.9 MPa<br>G: 0.7–3.6 Mg/m$^2$-s,<br>q''/G: < 0.34 kJ/kg<br>Flow orientation: →, ↑ |
| Razumovskiy et al., 1990 [43] | water | $Nu_b = \frac{(\xi_r/8) \bullet Re_b \bullet \overline{Pr_b}}{1.07 + 12.7 \bullet \sqrt{\xi_r/8} \bullet (\overline{Pr_b}^{2/3} - 1)} \bullet \left(\frac{\overline{c_p}}{cp_b}\right)^{0.35}$<br>$\xi_r = \xi_0 \bullet \left(\frac{\mu_w}{\mu_b}\right)^{0.18} \bullet \left(\frac{\rho_w}{\rho_b}\right)^{0.18}$ | d: 6.28 mm,<br>P: 23.5 MPa<br>G: 2.19 ton/m$^2$•s,<br>q'': 0.66–3.39 MW/m$^2$<br>Flow orientation: ↓ |

## References


[1] Z. Gu, H. Sato, Performance of supercritical cycles for geothermal binary design, Energy Convers. Manag. 43–7 (2002) 961–971, https://doi.org/10.1016/S0196-8904(01)00082-6.

[2] P. Garg, P. Kumar, K. Srinivasan, Supercritical carbon dioxide Brayton cycle for concentrated solar power, J. Supercrit. Fluids 76 (2013) 54–60, https://doi.org/10.1016/j.supflu.2013.01.010.

[3] C.S. Turchi, Z. Ma, T.W. Neises, M.J. Wagner, Thermodynamic study of advanced supercritical carbon dioxide power cycles for concentrating solar power systems, J. Sol. Energy Eng. 135–4 (2013), 041007, https://doi.org/10.1115/1.4024030.

[4] S.E. Bozbag, C. Erkey, Supercritical fluids in fuel cell research and development, J. Supercrit. Fluids 62 (2012) 1–31, https://doi.org/10.1016/j.supflu.2011.09.006.

[5] Y. Zhang, C. Erkey, Preparation of platinum-nafion-carbon black nanocomposites via a supercritical fluid route as electrocatalysts for proton exchange membrane fuel cells, Ind. Eng. Chem. Res. 44–14 (2005) 5312–5317, https://doi.org/10.1021/ie049177i.

[6] Y. Lin, X. Cui, C.H. Yen, C.M. Wai, PtRu/Carbon nanotube nanocomposite synthesized in supercritical fluid: a novel electrocatalyst for direct methanol fuel cells, Langmuir 21–24 (2005) 11474–11479, https://doi.org/10.1021/la051272o.

[7] M. Hoenig, D. Montgomery, Dense supercritical-helium cooled superconductors for large high field stabilized magnets, IEEE Trans. Magn. 11 (1975) 569–572, https://doi.org/10.1109/TMAG.1975.1058601.

[8] W.B. Bald, Supercritical helium cooling of hollow superconductors, in: K. D. Timmerhaus (Ed.), Advances in Cryogenic Engineering, vol. 16, Springer, 1971.

[9] C.C. Negoescu, Y. Li, B.A. Duri, Y. Ding, Heat transfer behaviour of supercritical nitrogen in the large specific heat region flowing in a vertical tube, Energy 134 (2017) 1096–1106, https://doi.org/10.1016/j.energy.2017.04.047.

[10] K. Yamagata, K. Nishikawa, S. Hasegawa, T. Fujii, S. Yoshida, Forced convective heat transfer to supercritical water flowing in tubes, Int. J. Heat Mass Tran. 15 (1972) 2575–2593, https://doi.org/10.1016/0017-9310(72)90148-2.

[11] S. Morkry, I. Pioro, P. Kirillove, Y. Gospodinov, Supercritical-water heat transfer in a vertical bare tube, Nucl. Eng. Des. 240 (2010) 568–576, https://doi.org/10.1016/j.nucengdes.2009.09.003.

[12] M.J. Watts, C.T. Chou, Mixed convection heat transfer to supercritical pressure water, Int. Heat Transfer Conf. München 3 (1982) 495–500, https://doi.org/10.1615/IHTC7.2970.

[13] J.M. Gopal, G. Tretola, R. Morgan, G.D. Sercey, A. Atkins, K. Vogiatzaki, Understanding sub and supercritical cryogenic fluid dynamics in conditions relevant to novel ultra low emission engines, Energies 13 (2020) 3038, https://doi.org/10.3390/en13123038.

[14] Y.Y. Bae, H.Y. Kim, D.J. Kang, Forced and mixed convection heat transfer to supercritical $CO_2$ vertically flowing in a uniformly-heated circular tube, Exp. Therm. Fluid Sci. 34 (2010) 1295–1308, https://doi.org/10.1016/j.expthermflusci.2010.06.001.

[15] Z.H. Li, P.X. Jiang, C.R. Zhao, Y. Zhang, Experimental investigation of convection heat transfer of $CO_2$ at supercritical pressures in a vertical circular tube, Exp. Therm. Fluid Sci. 34–8 (2010) 1162–1171, https://doi.org/10.1016/j.expthermflusci.2010.04.005.

[16] J.H. Song, H.Y. Kim, Y.Y. Bae, Heat transfer characteristics of a supercritical fluid flow in a vertical pipe, J. Supercrit. Fluids 44 (2008) 164–171, https://doi.org/10.1016/j.supflu.2007.11.013.

[17] D. Dimitrov, A. Zahariev, V. Kovachev, R. Wawryk, Forced convective heat transfer to supercritical nitrogen in a vertical tube, Int. J. Heat Fluid Flow 10 (1989) 1988–1990, https://doi.org/10.1016/0142-727X(89)90047-7.

[18] P. Zhang, Y. Huang, B. Shen, R.Z. Wang, Flow and heat transfer characteristics of supercritical nitrogen in a vertical mini-tube, Int. J. Therm. Sci. 50 (2011) 287–295, https://doi.org/10.1016/j.ijthermalsci.2010.06.014.

[19] H. Tatsumoto, Y. Shirai, K. Hata, T. Kato, M. Futakawa, M. Shiotsu, Forced convection heat transfer of subcooled liquid nitrogen in a vertical tube, J. Phys. Conf. 234 (2010), 032057, https://doi.org/10.1088/1742-6596/234/3/032057.

[20] I.L. Pioro, H.F. Khartabil, R.B. Duffey, Heat transfer to supercritical fluids flowing in channels—empirical correlations (survey), Nucl. Eng. Des. 230 (2004) 69–91, https://doi.org/10.1016/j.nucengdes.2003.10.010.

[21] C. Wang, H. Li, Evaluation of the heat transfer correlations for supercritical pressure water in vertical tubes, Heat Tran. Eng. 35 (6–8) (2014) 685–692, https://doi.org/10.1080/01457632.2013.837756.

[22] F. Li, B. Pei, B. Bai, Heat transfer correlations of supercritical fluids [online first], Intech (2019), https://doi.org/10.5772/intechopen.89356 available from: https://www.intechopen.com/online-first/heat-transfer-correlations-of-supercritical-fluids.

[23] Y. Wang, T.J. Lu, P. Drögemüller, Q.H. Yu, Y.L. Ding, Y.L. Li, Enhancing deteriorated heat transfer of supercritical nitrogen in a vertical tube with wire matrix insert, Int. J. Heat Mass Tran. 162 (2020), 120358, https://doi.org/10.1016/j.ijheatmasstransfer.2020.120358.

[24] J. Yang, Y. Oka, Y. Ishiwatari, J. Liu, J. Yoo, Numerical investigation of heat transfer in upward flows of supercritical water in circular tubes and tight fuel rod bundles, Nucl. Eng. Des. 237 (2007) 420–430, https://doi.org/10.1016/j.nucengdes.2006.08.003.

[25] S. He, W.S. Kim, J.D. Jackson, A computational study of convective heat transfer to carbon dioxide at supercritical pressure, Int. J. Therm. Sci. 44–6 (2005) 521–530, https://doi.org/10.1016/j.ijthermalsci.2004.11.003.

[26] Y.Y. Bae, E.S. Kim, M. Kim, Numerical simulation of upward flowing supercritical fluids using buoyancy-influence-reflected turbulence model, Nucl. Eng. Des. 324–1 (2017) 231–249, https://doi.org/10.1016/j.nucengdes.2017.08.026.

[27] F.W. Dittus, L.M.K. Boelter, Heat transfer in automobile radiators of the tubular type, Univ. Calif. Publ. Entomol. 2 (1930) 443–461.

[28] S.H. Yoon, J.H. Kim, Y.W. Hwang, M.S. Kim, K. Min, Y. Kim, Heat transfer and pressure drop characteristics during the in-tube cooling process of carbon dioxide in the supercritical region, Int. J. Refrig. 26–8 (2003) 857–864, https://doi.org/10.1016/S0140-7007(03)00096-3.

[29] H.S. Swenson, J.R. Carver, C.R. Kakarala, Heat transfer to supercritical water in smooth-bore tubes, J. Heat Tran. 87–4 (1965) 477–484, https://doi.org/10.1115/1.3689139.

[30] A.A. Bishop, R.O. Sandberg, L.S. Tong, Forced convection heat transfer to water at near-critical temperatures and supercritical pressure, Am. Inst. Chem. Engrs.-I. Chem. E. Symposium Series No.2, London Instn. Chem. Engrs. WCAP-2056-P (Part-III-B) (1965) 1–28.

[31] J.D. Jackson, W.B. Hall, Forced convection heat transfer to fluids at supercritical pressure, in: Turbulent Forced Convection in Channels and Bundles vol. 2, Hemisphere, New York, NY, 1979, pp. 563–611.

[32] L.M. Gorban, R.S. Pometko, Modeling of Water Heat Transfer with Freon of Supercritical Pressure, Institute of Physics and Power Engineering, Obninsk, Russia, 1990.

[33] B. Kuang, Y. Zhang, X. Cheng, A wide-ranged heat transfer correlation of water at supercritical pressures in vertical upward tubes, in: Proceedings of the China-Canada Joint Workshop on SCWR, 2008. Shanghai, China.

[34] Y.Y. Bae, H.Y. Kim, Convective heat transfer to $CO_2$ at a supercritical pressure flowing vertically upward in tubes and an annular channel, Exp. Therm. Fluid Sci. 33 (2009) 329–339, https://doi.org/10.1016/j.expthermflusci.2008.10.002.

[35] S. Mokry, I.L. Pioro, A. Farah, K. King, S. Gupta, W. Peiman, Development of supercritical water heat-transfer correlation for vertical bare tubes, Nucl. Eng. Des. 241 (2011) 1126–1136, https://doi.org/10.1016/j.nucengdes.2010.06.012.

[36] J.D. Jackson, Fluid flow and convective heat transfer to fluids at supercritical pressure, Nucl. Eng. Des. 264 (2013) 24–40, https://doi.org/10.1016/j.nucengdes.2012.09.040.

[37] V.I. Deev, V.S. Kharitonov, A.M. Baisov, A.N. Churkin, Universal dependencies for the description of heat transfer regimes in turbulent flow of supercritical fluids in channels of various geometries, J. Supercrit. Fluids 135 (2018) 160–167, https://doi.org/10.1016/j.supflu.2018.01.019.

[38] V. Gnielinski, New equations for heat and mass transfer in turbulent pipe and channel flow, Int. Chem. Eng. 16 (1976) 359–368.

[39] W. Chen, X. Fang, Y. Xu, X. Su, An assessment of correlations of forced convection heat transfer to water at supercritical pressure, Ann. Nucl. Energy 76 (2015) 451–460, https://doi.org/10.1016/j.anucene.2014.10.027.

[40] H. Zahlan, S. Tavoularis, D.C. Groeneveld, A look-up table for trans-critical heat transfer in water-cooled tubes, Nucl. Eng. Des. 285 (2015) 109–125, https://doi.org/10.1016/j.nucengdes.2014.12.027.

[41] E.A. Krasnoshchekov, V.S. Protopopov, Heat transfer at supercritical region in flow of carbon dioxide and water in tubes (in Russian), Therm. Eng. 12 (1959) 26–30.

[42] B.S. Petukhov, V.A. Kurganov, V.B. Ankudinov, Heat transfer and flow resistance in the turbulent pipe flow of a fluid with near-critical state parameters, High Temp. 21 (1983) 81–89.

[43] V.G. Razumovskiy, A.P. Ornatskiy, Y.M. Mayevskiy, Local heat transfer and hydraulic behavior in turbulent channel flow of water at supercritical pressure, Heat Tran. Sov. Res. 22–1 (1990) 91–102.

[44] Z. Wang, R. Xu, C. Xiong, P. Jiang, Experimental study on the inhibition of heat transfer deterioration of supercritical pressure $CO_2$, J. Tsinghua Univ. (Sci. Technol.) 58 (2018) 1101–1106, https://doi.org/10.16511/j.cnki.qhdxxb.2018.25.046.

[45] S. Gupta, E. Saltanov, S.J. Mokry, I. Pioro, L. Trevani, D. McGillivray, Developing empirical heat-transfer correlations for supercritical $CO_2$ flowing in vertical bare tubes, Nucl. Eng. Des. 261 (2013) 116–131, https://doi.org/10.1016/j.nucengdes.2013.02.048.

[46] G. Richards, G.D. Harvel, I.L. Pioro, A.S. Shelegov, P.L. Kirillov, Heat transfer profiles of a vertical, bare, 7-element bundle cooled with supercritical Freon R-12, Nucl. Eng. Des. 264 (2013) 246–256, https://doi.org/10.1016/j.nucengdes.2013.02.019.

[47] H. Cheng, L. Yin, Y. Ju, Y. Fu, Experimental investigation on heat transfer characteristics of supercritical nitrogen in a heated vertical tube, Int. J. Therm. Sci. 152 (2020), 106327, https://doi.org/10.1016/j.ijthermalsci.2020.106327.


## Nomenclature

### Latin symbols

*Bu:* buoyancy parameter, $\overline{Gr_b}/Re_b^{2.7}$
*$C_p$:* specific heat, J/kg-K
*$\overline{c_p}$:* average specific heat between bulk core and tube wall, J/kg-K
*$CO_2$:* carbon dioxide
*d:* diameter, mm
*E:* Eckert number
*$F_c$:* correction factor
*G:* mass flux, kg/m$^2$-s
*Gr:* Grashof number
*$\overline{Gr_b}$:* average Grashof number between bulk core and tube wall
*Gr*:* non-dimensional effective Grashof number h
*H:* specific enthalpy, kJ/kg

*HTC:* heat transfer coefficient, W/m$^2$-K
$H_{in}$: inlet specific enthalpy, kJ/kg
*ID:* tube inner diameter
*k:* thermal conductivity, W/m-K
$K_h$: criterion of thermal acceleration
$K_{Am}$: enthalpy criterion L
*MAPE:* mean absolute percentage error
*RMSPE:* root mean squared percentage error
$N_2$: nitrogen
*Nu:* Nusselt number
*P:* pressure, Pa
*Pr:* Prandtl number
$\overline{Pr_b}$: average Prandtl number between bulk core and tube wall
*PEC:* performance enhancement index
$\Delta P$: pressure drop, Pa
*Re:* Reynolds number
*T:* temperature, °C
*U:* dependent variable
*x:* local axial location, mm
$\Delta x$: tube wall thickness, mm
*X:* tube wall thickness, m
$X_n$: n$^{th}$ independent variable
*Y:* correction factor
$q^{"}$: heat flux, W/m$^2$
$q^+$: non-dimensional effective heat flux heat transfer coefficient, W/m$^2$-K

## Greek symbols

$\eta$: performance enhancement index
$\sigma$: uncertainty of a certain variable
$\lambda$: thermal conductivity, W/m-K
$\rho$: density, kg/m$^3$
$\mu$: dynamic viscosity, Pa•s
*length:* m

## Subscripts

*b:* bulk fluid
*basic:* plain test tube without insert
*c:* critical point
*enhanced:* test tube with insert
*in:* tube inner
*local:* local value along test tube axis
*n:* empirical index
*pc:* pseudo-critical point
*v:* vapor-like phase
*w:* tube wall